TRI-BAND OBJECT-RESISTANT ANTENNA DESIGN

A Thesis
Presented to
The Academic Faculty

by

Tianchong Jiang

In Partial Fulfillment
of the Requirements for the Degree
Master of Science in the
School of Electrical and Computer Engineering

Georgia Institute of Technology
December 2018

TRI-BAND OBJECT-RESISTANT ANTENNA DESIGN

Approved by:

Dr. Gregory D. Durgin, Advisor
School of Electrical and Computer Engineering
Georgia Institute of Technology

Dr. Andy Peterson
School of Electrical and Computer Engineering
Georgia Institute of Technology

Dr. Waymond Scott
School of Electrical and Computer Engineering
Georgia Institute of Technology

Date Approved: August 23, 2018

ACKNOWLEDGEMENTS

I would like to thank my advisor, Dr. Gregory Durgin, who first got me interested in antenna design and has been supporting me at every step in the process. I would also like to thank the members of my lab, particularly Cheng Qi, whose expertise and creativity helped me fix a lot of problems when designing the antenna.

Finally, I would like to thank my parents, who support me to go further study in Georgia Tech.

TABLE OF CONTENTS

LIST OF TABLES

LIST OF FIGURES

LIST OF SYMBOLS AND ABBREVIATIONS

RFID	Radio-Frequency Identification
NFC	Near-Field Communication
WLAN	Wireless Local Area Network
LTE	Long-Term Evolution
ISM	Industrial, Scientific, and Medical
PIFA	Planar Inverted F-antenna

SUMMARY

A new tri-band monopole antenna is proposed in this thesis. The antenna is made up of two simple L-shaped structures making it easy to fabricate and low in cost. The three target ISM bands (915MHz, 2.4GHz and 5.8GHz) enable it to be used for for low-power and short range telecommunications, such as WiFi, Bluetooth, Zigbee, wireless telephones, RFID, and NFC links. The bandwidths are designed to be in excess of the allotted bands making the antenna resistant to the presence of nearby object variations. This allows the antenna design to be used across the broadest possible application space.

The proposed antenna is fabricated on an 80mm * 80mm RO4730 board and achieves a bandwidth of 9.3%, 66.7% and 12.4% at 915MHz, 2.4GHz, and 5.8GHz respectively. For the antenna gain, it achieves 2.5dBi, 4dBi and 4.3dBi at 915MHz, 2.4GHz and 5.8GHz respectively.

CHAPTER 1. INTRODUCTION

In wireless communications, there is an increasing need to manufacture multi-band antennas with small size, low cost and easy fabrication to integrate into everyday devices. For many multi-band antennas, the designs are based on an inverted F-shaped structure because of its small size and low profile [1]. These designs usually make use of adding slots or branches to the basic planar design. However, in order to make the antenna work at multiple bands, very complex structures must be introduced into the design of an F-shaped antenna [1]. Compared to an inverted F-structure, the proposed antenna is built with a simpler L-structure and uses Rogers RO4730 as the dielectric material to minimize loss. The antenna is supposed to work at three ISM bands, 915MHz, 2.4GHz, and 5.8GHz and the antenna will be suited for low-power and short range telecommunications, such as WiFi, Bluetooth, Zigbee, wireless telephones, RFID, and NFC links.

In order to allow the proposed antenna to be used across the broadest set of environments, all of three parts of the antenna are designed to be broadband for the purpose of being resistant to the presence of nearby objects. Since antennas can be placed in a variety of form factors and environments, the presence of varied conductors and dielectrics will de-tune and alter the radiation pattern. Thus, not only do we seek a tri-band antenna, but one that resists the presence of nearby object variations. This will allow a single antenna design to be used across the broadest possible application space. In order to accomplish this, the antenna should have a wide bandwidth so that its performance is not severely affected even after detuning due to material proximity [2]. More related experiments can be found in [3], where the performance of any antenna degrades whenever various

dielectric materials are brought in close proximity, similar to the RFID-style antennas observed and categorized by Griffin.

1.1 Multi-band Antenna

1.1.1 Dual-band Antenna

Since dual-band antennas are simpler than tri-band antennas, there are more dual-band antenna designs in the research literature. For most of them, the antennas are designed to operate in the WLAN frequencies (2.4GHz/5.8GHz) [4], LTE frequencies (400MHz – 4GHz) [5], and 5G communication bands [4], [6].

For the WLAN and 5G applications in Japan, a dual-band miniaturized planar inverted F-antenna(PIFA) can achieve a return loss of -18dB at 2.5GHz(LTE2500) with a bandwidth of about 310MHz and a return loss of -33dB at 4.5GHz(5G) with a bandwidth of about 220MHz, respectively [4]. There are also other kinds of dual-band antenna for WLAN application. More specifically, for WiFi, a miniaturized tapered meandered dual-band dipole antenna is designed to work at 2.4GHz and 5.8GHz. Although the size is very small, the structure is quite complex [7]. For these reconfigurable antennas, they are explored in the research literature as a way to enhance bandwidth or bands of operation, but require extra RF ports or RF electronic components which add loss, cost and complexity.

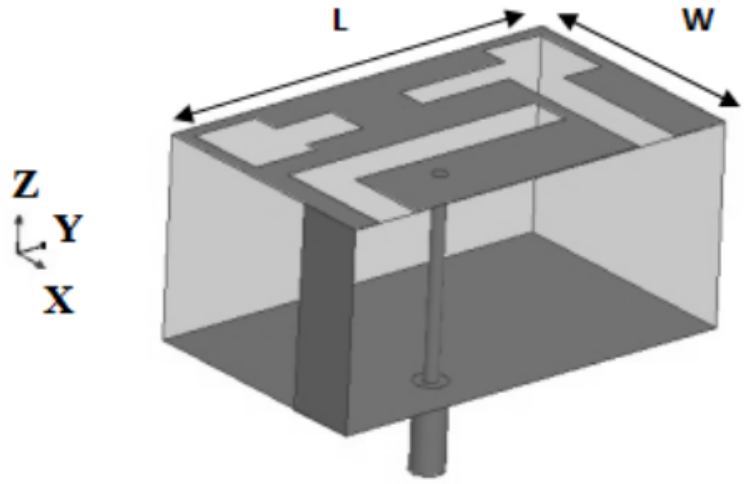

Figure 1 – The configuration of slotted PIFA in [4]

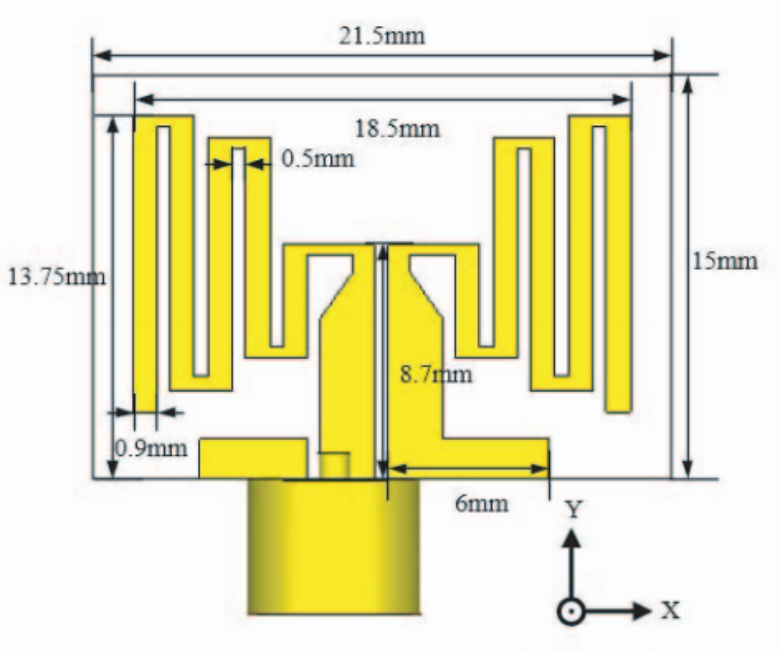

Figure 2 – Detailed configuration of the proposed antenna in [7]

1.1.2 Tri-band Antenna

For tri-band antennas, the working frequencies are similar to dual-band ones. However, the structures are more complicated: In [8], a four-layer stacked tri-band microstrip patch antenna was proposed to work 1.66GHz, 3.25GHz and 5.27GHz and achieved a bandwidth of 3%, 3% and 18% at each band, respectively. For this design, the antenna has four layers so it would take more effort to be manufactured. In contrast, a multiband planar inverted F antenna was designed to cover both GSM and DCS bands in [9]. The proposed antenna featured a rectangular patch antenna for GSM (880-960MHz) band and an F-shaped slot antenna for DCS (1710-1880MHz) and GSM (1710-1880MHz) bands. It has a flat structure and is easy to manufacture on a two-layer PCB.

1.2 L-shaped Antenna

In order to make the proposed antenna structure flat and simple, an L-shaped antenna is selected. The L-shaped antenna is one of the common structures in antenna design and it can be designed to generate broad bandwidth.

In [10], an L-shaped printed monopole antenna was proposed for wide bandwidth and dual linear polarization. The simulated bandwidth ratio is 3.9:1, which is a very useful range for many communication bands.

In [11], a print monopole dual-band antenna was designed to operate to work at 2.4/5.2 GHz, and its obtained bandwidth (1: 1.5 VSWR) reached 390 MHz (2300-2690 MHz) and 650 MHz (4830-5480 MHz) for the lower and upper operating bands, respectively.

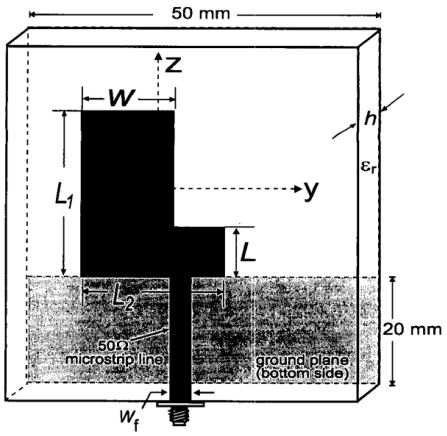

Figure 3 – Geometry of microstrip-fed printed L-shaped monopole in [11]

1.3 Microstrip Antenna

The microstrip antennas are used for the design of the proposed tri-band antenna in this thesis and they are chosen for their ease of analysis and fabrication and attractive radiation characteristics, especially low cross-polarization radiation. Besides, they are also low profile, conformable to planar and nonplanar surfaces, simple and inexpensive to fabricate using modern printed-circuit technology, mechanically robust when mounted on rigid surfaces, compatible with MMIC designs, and very versatile in terms of resonant frequency, polarization, pattern, and impedance [12].

1.4 ISM Band

The proposed antenna, is targeting the 915MHz, 2.4GHz and 5.8GHz bands, a series of unlicensed UHF microwave bands used around the world. It can be seen from above that, it is very common to make dual-band antennas that operate at 2.4GHz and 5.8GHz. Hence, 915MHz is added to the proposed antenna.

The industrial, scientific and medical (ISM) radio bands are radio bands (portions of the radio spectrum) reserved internationally for the use of radio frequency (RF) energy for industrial, scientific and medical purposes other than telecommunications [13].

For the range of 902MHz ~ 928MHz the center frequency is 915MHz. This ISM band is available in ITU region 2 only. This band is commonly used for wireless links for short-range audio and video transmission, as well as a variety of remote control, metering and sensing applications [14].

For the range of 2.4GHz ~ 2.5GHz the center frequency is 2.45GHz. This band is available worldwidely although there is some minor variation at the very ends of the bands. This band is commonly used for cordless telephones, monitors, bluetooth and Wi-Fi - 802.11b/g wireless networking [15].

For the range of 5.725GHz ~ 5.875GHz the center frequency is 5.8GHz. It is available worldwidely. This band is commonly used for Wi-Fi - 802.11a/n/ac wireless networking.

All of the frequency bands are type B, according to [9]; namely all their frequency bands are also designated for ISM applications. Radio communication services operating within these bands must accept the presence of potentially harmful interference which may be caused by these applications [16].

Table 1– ISM Licensed Users [16]

Center Frequency	Licensed Users
915MHz	FIXED, Mobile except aeronautical mobile & Radiolocation service; in Region 2 additional Amateur service
2.45GHz	FIXED, MOBILE, RADIOLOCATION, Amateur & Amateur-satellite service
5.8GHz	FIXED-SATELLITE, RADIOLOCATION, MOBILE, Amateur & Amateur-satellite service

CHAPTER 2. ANTENNA DESIGN

2.1 Dual-band Antenna Design

Before designing the proposed tri-band antenna, a dual-band object-resistant antenna was first designed. On the basis of the dual-band antenna, it will be easier to design the proposed tri-band antenna.

For the initial dual-band antenna, the working frequencies are 2.4GHz and 5.8GHz. In order to make the antenna object resistant, its bandwidth should be in excess of its allotted band. More specifically, the bandwidth should be more than 10% of the working frequency: e.g. for 2.4GHz the bandwidth should be at least 0.24GHz. In this part, two L-shaped microstrip antennas were used for the design. The design in [17] shows a good example of a dual-band planar monopole antenna with two L-shaped antennas.

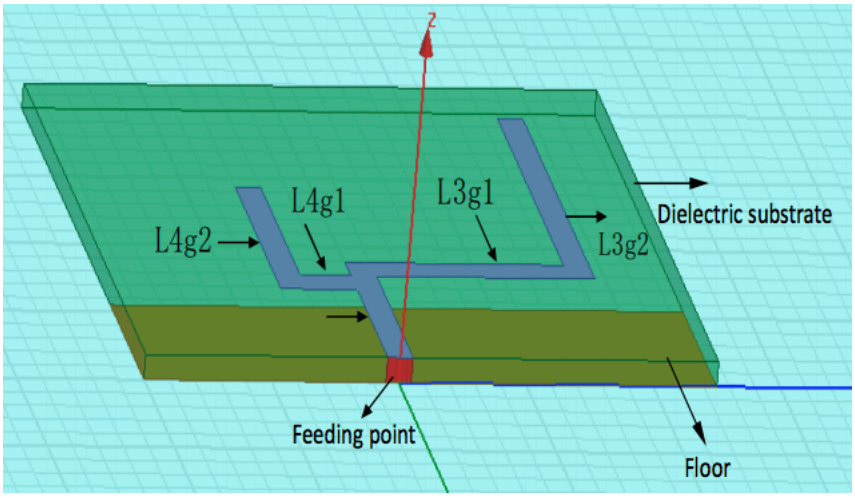

Figure 4 – The 3D model of the dual-band antenna in [17]

Rogers RO4003 is selected as the dielectric material. Its relative permittivity is 3.38 and its dielectric loss tangent is 0.0027. According to the design in [17], an ideal antenna

is first simulated in ANSYS HFSS, which means it has no thickness and its boundary is assigned as perfect conductor (Perfect E in HFSS). Then the lengths of the L-shaped antennas are changed to obtain the target frequencies, namely 2.4GHz and 5.8GHz.

It can be seen in Figure 5 that the left L structure is a monopole antenna that works at 5.8GHz. In free space propagation the wavelength of 5.8GHz is 52mm. In the dielectric material, the wavelength is 28mm. We design a 1/4 wavelength monopole antenna. So after calculation, the length of the antenna should be between 7mm and 13mm. Similarly, the right L structure is a monopole antenna that works at 2.4GHz. In free space propagation the wavelength of 2.4GHz is 125mm. In the dielectric material, the wavelength is 68mm. We design a 1/4 wavelength monopole antenna. So after calculation, the length of the antenna should be between 17mm and 31mm.

After initial design, the optimization process is performed with the Optimetics function in HFSS. Since the resonance frequency varies inversely with the length of the L-shaped antenna, the length of L1, L2, R1 and R2 are adjusted to produce the target frequencies. The detailed simulation process will be discussed in Section 2.3.

The final design configuration is shown in Figure 4. The left L-shaped antenna contributes to the 5.8GHz frequency and the right one contributes to 2.4GHz. The design properties are shown in Table 2 in Appendix A. The total length of the left antenna is 11.25mm which is in the range of 7mm and 13mm; and the total length of the right antenna is 29.25mm which is in the range of 17mm and 31mm. Both of them accord with the previous calculation.

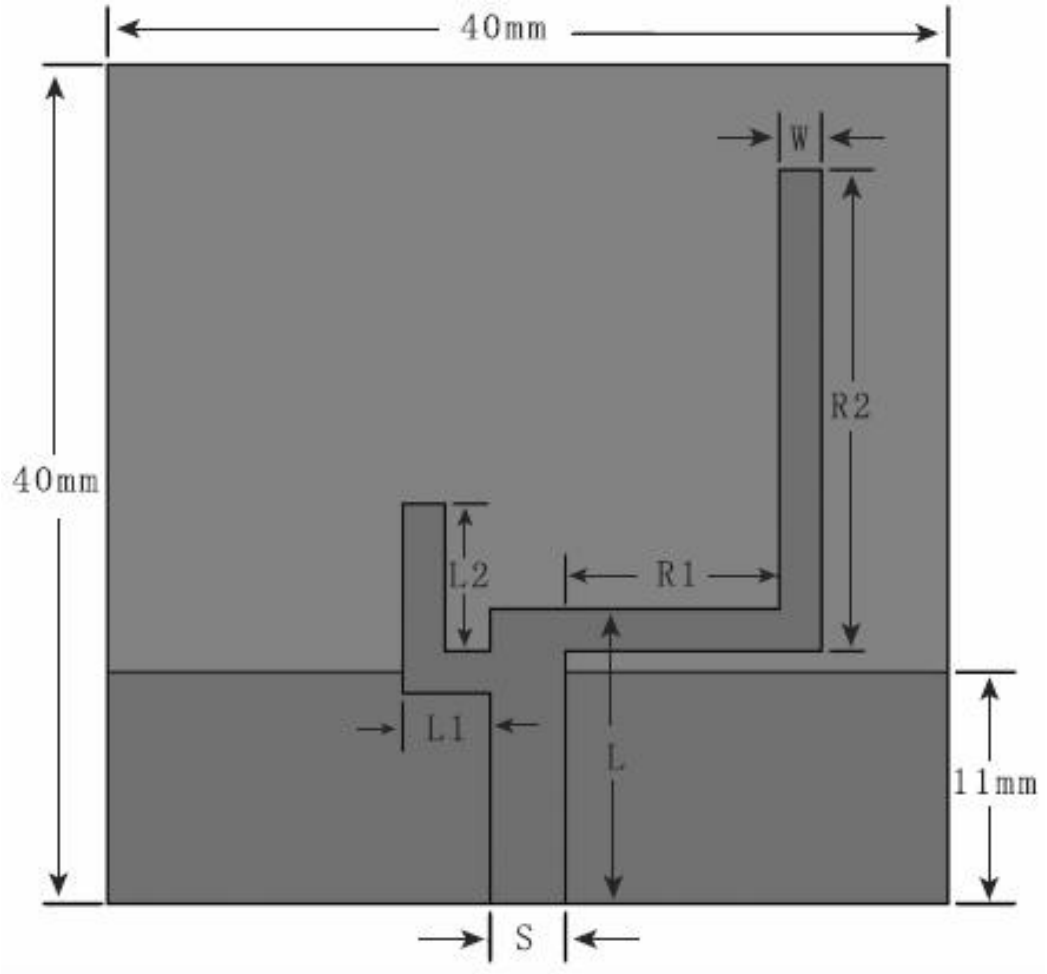

Figure 5 – Configuration of the proposed dual-band antenna

The simulation result shows that for -10dB bandwidth, the lower band(2.4GHz) ranges from 2.24GHz to 2.84GHz and the upper band(5.8GHz) ranges from 4.96GHz to over 7.3GHz. The bandwidth ratio is 4: 1 for 2.4GHz and 2.48: 1, which means the bandwidth is broad enough for object-resistant applications. If an object of significant permeability and/or conductivity approaches the antennas, the resonances will begin to shift in the frequency domain. However, the additional achieved bandwidth provides a sufficient “margin of error” for this type of de-tuning.

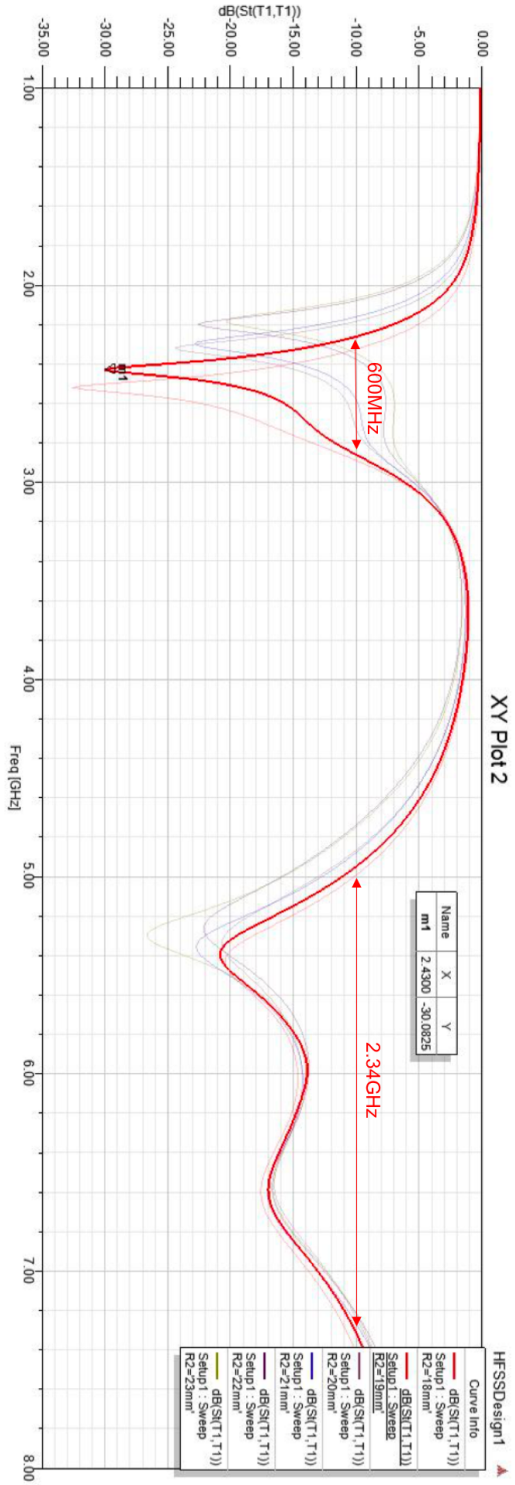

Figure 6 – S-Parameter(S11) of the proposed dual-band antenna (-10dB bandwidth)

2.2 Design Process

2.2.1 Basic Design

The target of this project is to design a tri-band compact antenna which should also satisfy the need of object-resistance. So the design could also be divided into two parts: First, design a tri-band antenna working at the proposed frequencies. Second, make the bandwidth of the antenna in excess of its allotted band.

Also, the goal of the design is to make the antenna simple and easy to manufacture, so three L-shaped microstrip antennas are proposed for the tri-band applications. The dual-band antenna design has already shown that the L-shaped antennas can work well for broadband. Rogers RO4730 is selected as the dielectric material. Its relative permittivity is 3 and its dielectric loss tangent is 0.0023.

The left L structure should be a monopole antenna that works at 2.4GHz. In free space propagation the wavelength of 2.4GHz is 125mm. In the dielectric material, the wavelength at 2.4GHz drops to 72mm. To make a 1/4 wavelength monopole antenna, the antenna should be 1/4 of the wavelength. So after calculation, the length of the antenna should be between 18mm and 31mm.

The right upper L structure should be a monopole antenna that works at 5.8GHz. In free space propagation the wavelength of 5.8GHz is 52mm. In the dielectric material, the wavelength drops to 30mm. After calculation, the length of the antenna should be between 7.5mm and 13mm.

The right lower L structure should be a monopole antenna that works at 915MHz. In free space propagation the wavelength of 915MHz is 328mm. In the dielectric material, the wavelength drops to 189mm. After calculation, the length of the antenna should be between 47.3mm and 82mm.

2.2.2 Simulation and Optimization Process

For this design, all the simulations and optimizations are performed in ANSYS HFSS. In the design of the dual-band antenna above, the ground of the antenna was set as an ideal conductor boundary (perfect E). However, in the tri-band antenna design, in order to get more precise simulation results, the ground of antenna is set to be copper in the simulation with thickness of 35um. Then, the radiation boundary conditions can be set according to the size of the antenna, and the distance between the radiation surface and the radiators need be no less than 1/4 wavelength. So, the distance between the antenna and the air box where the radiation field is established is set to 100mm (longer than 82mm). The lumped port excitation is set in the YZ plane of the model with the port referenced to ground. After setting up the solution frequency and analyzing of the grid, the performance of the dual band planar monopole antenna was simulated under ANSYS HFSS.

Based on the influence of the size of the antenna on the antenna performance of S-Parameter(S11), the sizes of all the three L-shaped antennas have been analyzed. At the first stage, only the length of the antennas is adjusted. One example is given in Figure 7: it is hard to satisfy our three target frequencies simultaneously. For the design in Figure 7, the S-Parameter(S11) at 915MHz and 2.4GHz is below -10dB, which meets our

requirements, but the S11 for 5.8GHz is over -10dB. Also, the band is quite narrow for 915MHz.

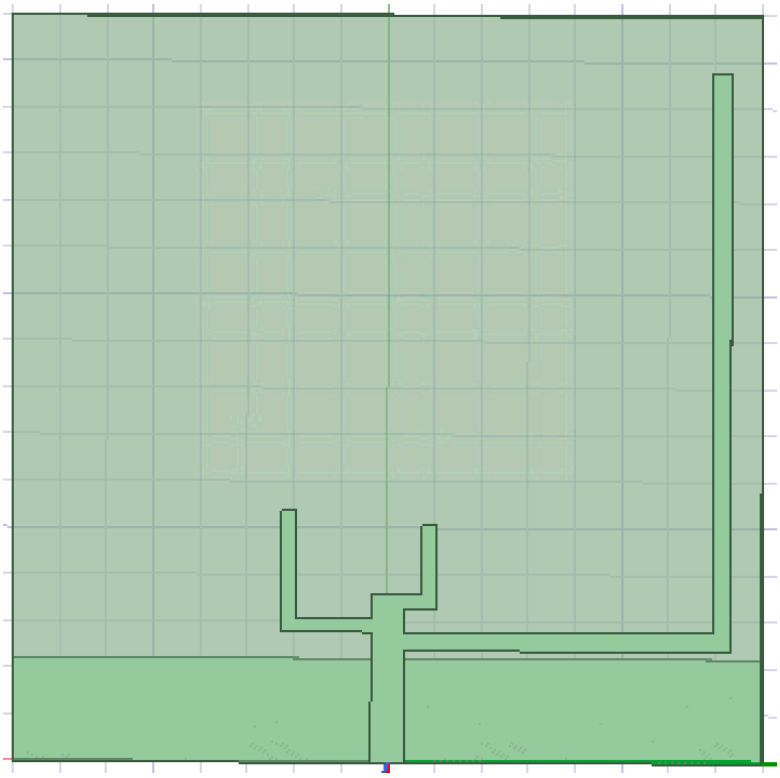

Figure 7 – Configuration of an example with three L-shaped structures

The geometry was adjusted for the next design iteration. The width of the antennas is taken into consideration. After several optimization steps, the 5.8GHz monopole shrinks into a very small antenna as shown in Figure 9. A bigger L-shaped antenna will influence the performance of the other two working frequencies, especially the 915MHz band. However, since a small L-shaped antenna will not have much effect for the whole design, the simulation and optimization results lead to a conclusion that there is no need to build an L-shaped antenna for 5.8GHz. So this part of the antenna is removed in the final design.

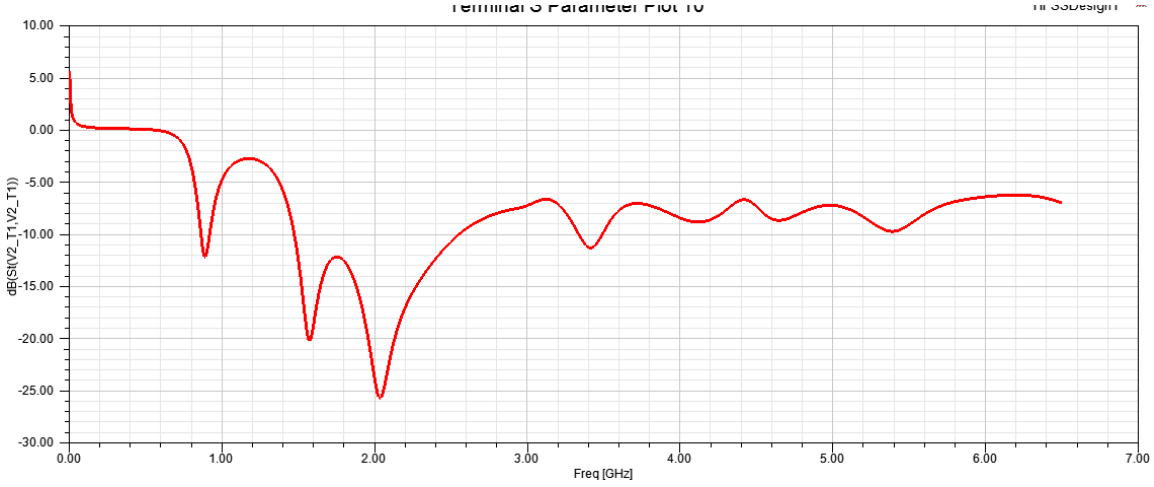

Figure 8 – S-Parameter(S11) of the antenna in Figure 7

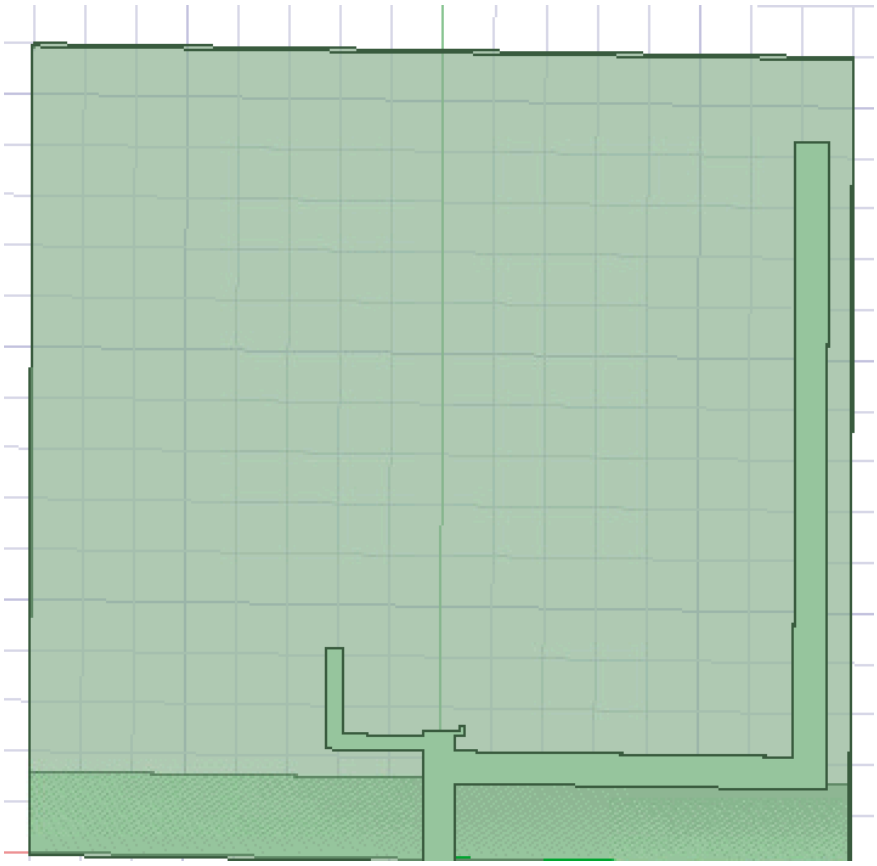

Figure 9 – Configuration of an example with a tiny L-shaped structure for 5.8GHz

2.3 Final Design

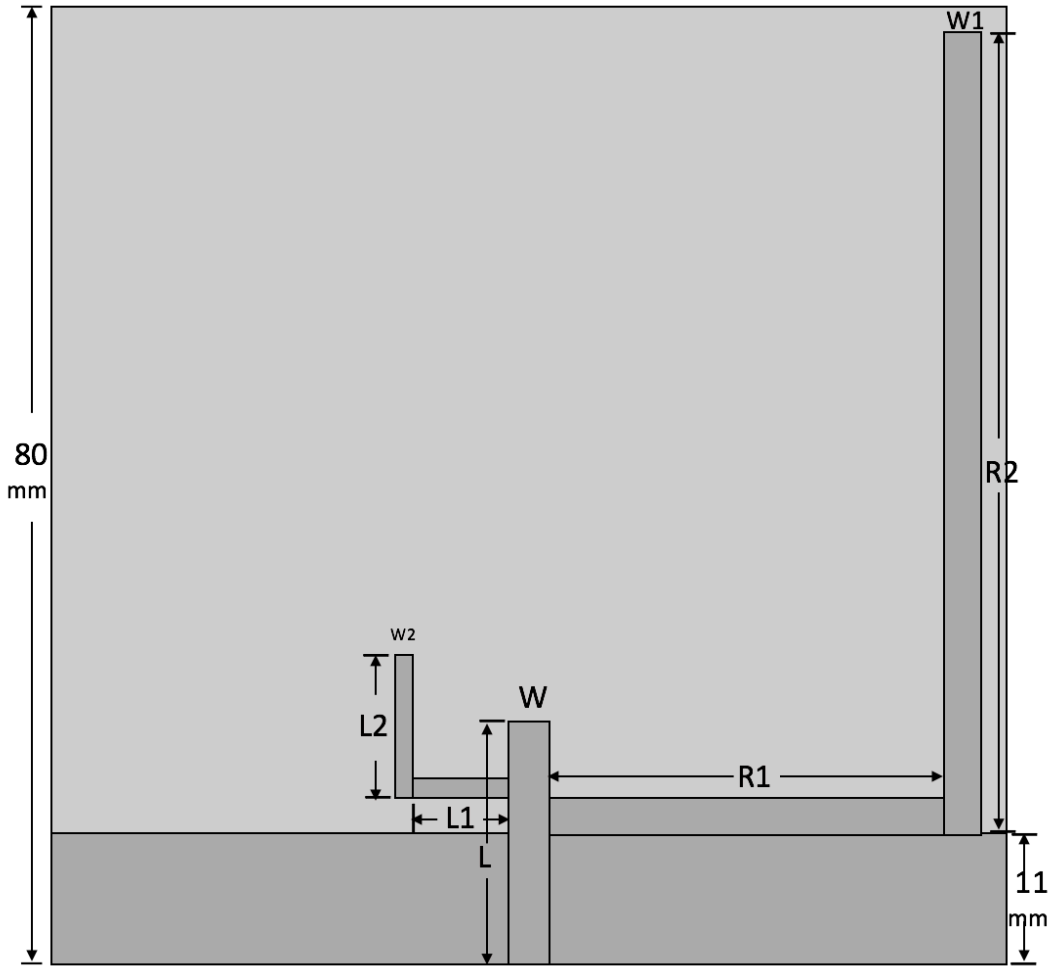

Figure 10 – Final version of the proposed antenna

After some minor optimization for the length and width of the two L-shaped antennas, the final parameters of the tri-band antenna have changed. For the right L-shaped antenna, the horizontal length (R1) is 33mm, the vertical length (R2) is 67mm and the width (W1) is 3.1mm. For the left L-shaped antenna, the horizontal length (L1) is 8mm, the vertical length (L2) is 12mm and the width (W2) is 1.5mm. Accordingly, the whole antenna board grows into an 80mm*80mm square.

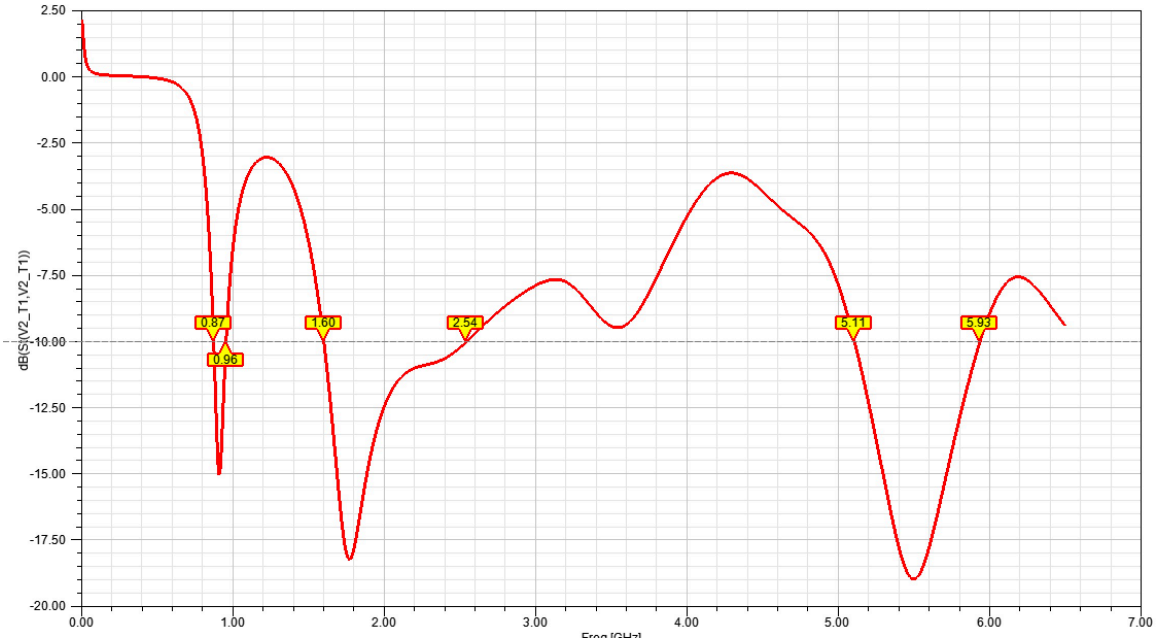

Figure 11 – S-Parameter(S11) of the proposed antenna in Figure 10

The simulation result is shown in Figure 11. For all of the working frequencies, the S-Paremeter (S11) is lower than -10dB, which satisfies our need. For the target frequency of 915MHz, the band ranges from 870MHz to 960MHz, making a bandwidth of 90MHz and a bandwidth ratio of 9.8%. For the target frequency of 2.4GHz, the band ranges from 1.6GHz to 2.54GHz, making a bandwidth of 0.94GHz and a bandwidth ratio of 34.1%. For the target frequency of 5.8GHz, the band ranges from 5.11GHz to 5.93GHz, making a bandwidth of 0.82GHz and a bandwidth ratio of 14.1%. In conclusion, for the simulation part, the proposed antenna can operate at the required frequencies. For 2.4GHz and 5.8GHz, it is no doubt broadband, but for 915MHz, the bandwidth may not be wide enough.

In order to do further research, the total realized gain is simulated in HFSS. From Figures 12, 13, 14, 15, 16, and 17, the peak gain for 915MHz, 2.4GHz and 5.8GHz is 2dBi, 3dBi and 5dBi. For 915MHz and 2.4GHz, the antenna is more omni-directional. For

5.8GHz the radiation pattern is scalloped. That accords with the fact that only two L-shaped structures are adopted for 915MHz and 2.4GHz. Since there is no specific L-shaped antenna designed for 5.8GHz, the 5.8GHz performance may be degraded by the harmonic frequencies generated by the 915MHz, 2.4GHz antennas and the feeder line. In the thesis process, it is figured out that it is hard to meet the targeting frequencies and the object-resistance with three L-shaped antennas. So to avoid the scalloped pattern of the 5.8GHz some other design could be introduced. This further optimization is left a topic of our future research.

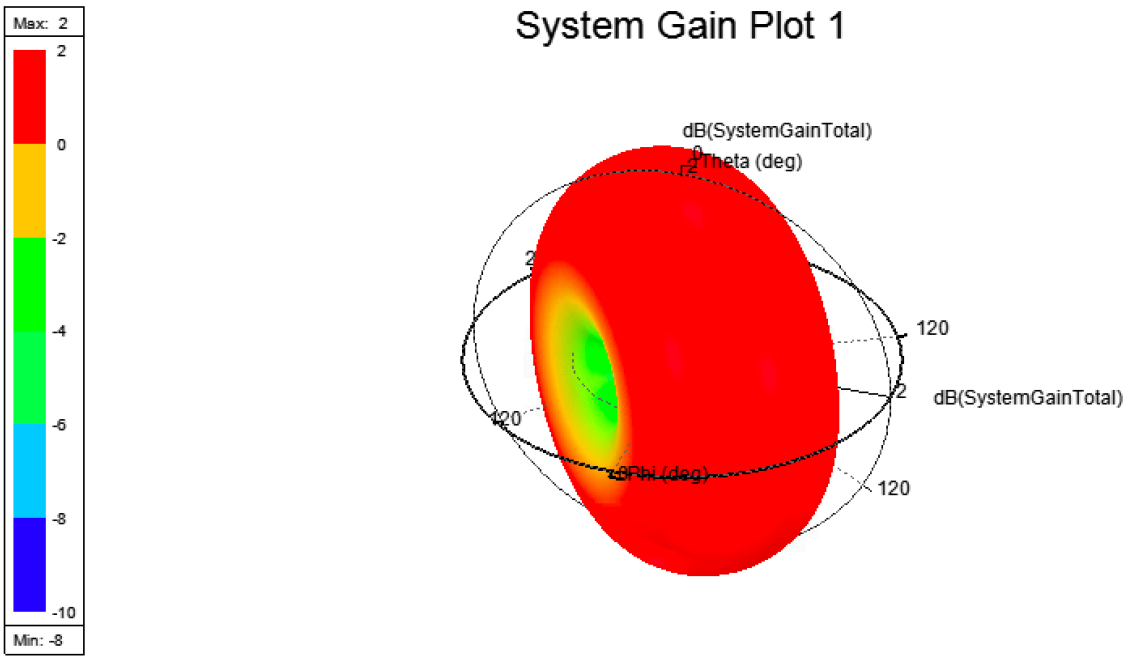

Figure 12 – Realized gain for 915MHz (Peak Gain 2dBi)

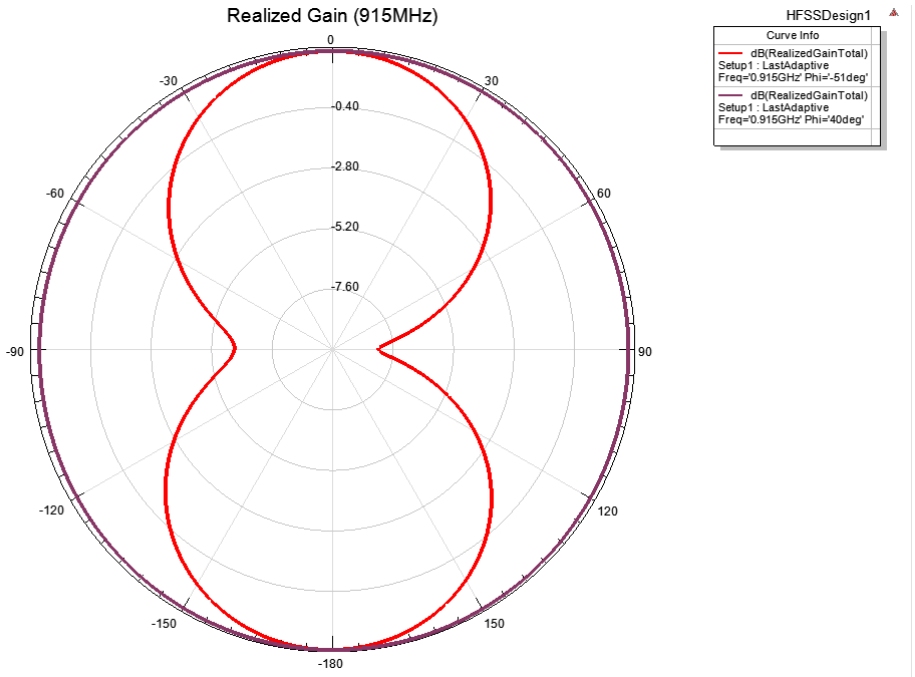

Figure 13 – Radiation pattern for 915MHz (purple trace for E-Plane and red trace for H-Plane)

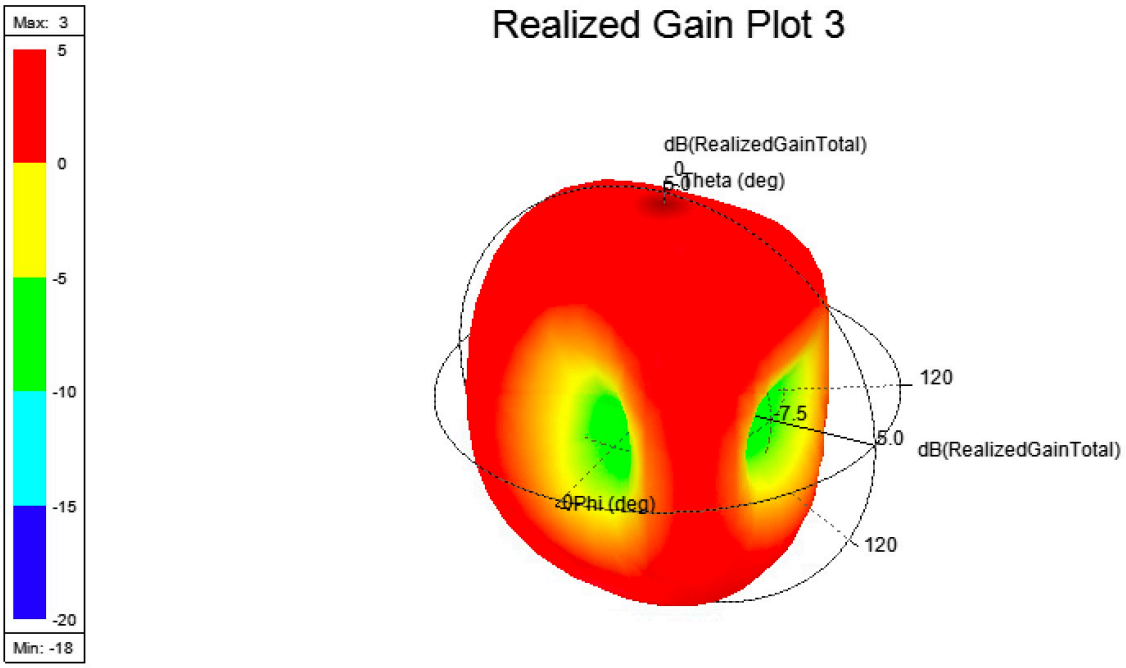

Figure 14 – Realized gain for 2.4GHz (Peak Gain 3dBi)

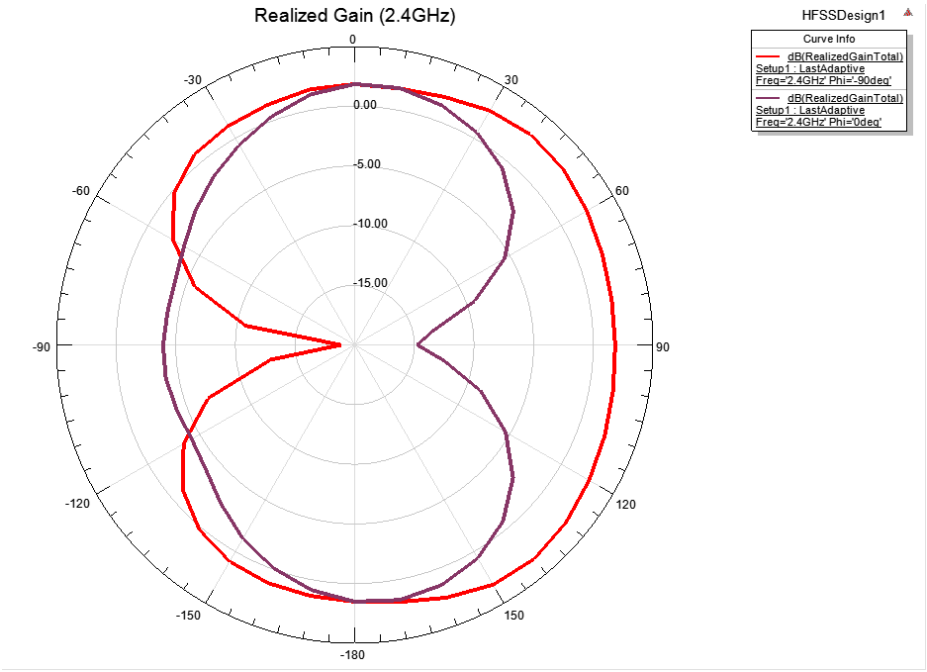

Figure 15 – Radiation pattern for 2.4GHz 8GHz (red trace for E-Plane and purple trace for H-Plane)

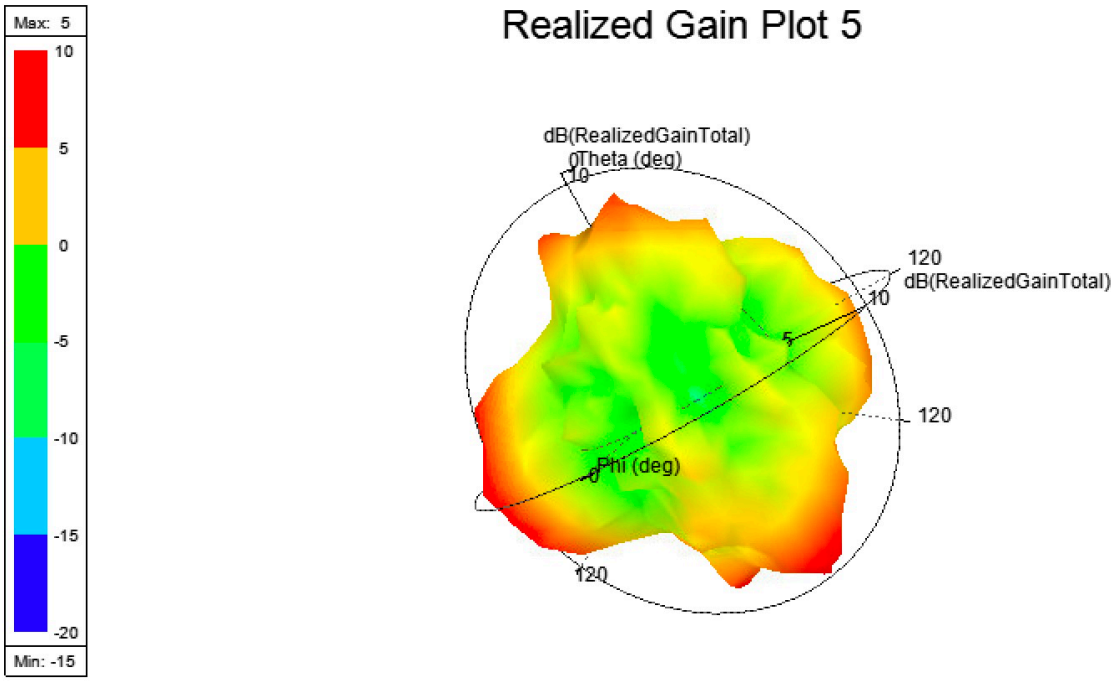

Figure 16 – Realized gain for 5.8GHz (Peak Gain 5dBi)

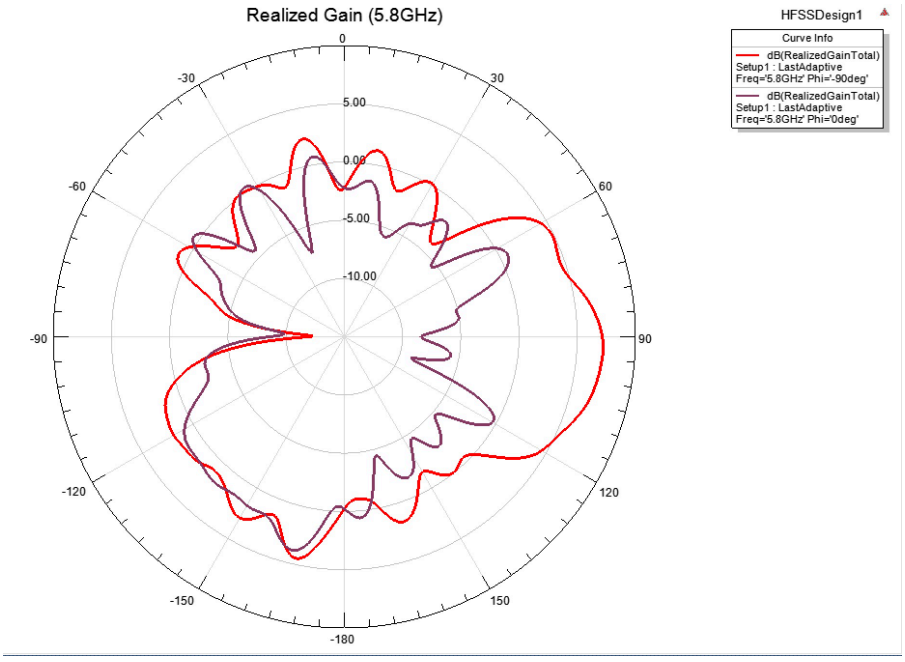

Figure 17 – Radiation pattern for 5.8GHz (red trace for E-Plane and purple trace for H-Plane)

CHAPTER 3. FABRICATION AND TESTING

3.1 Fabrication Process

The layout of the printed circuit board is performed in Autodesk Eagle. Figure 18 is the view of the board file. The blue part at the bottom shows the solid ground plane and the antenna is fed by the SMA-to-microstrip connector from the bottom of the red antenna. The feed port and the ground plane can be seen more clearly in Figures 19 and 20.

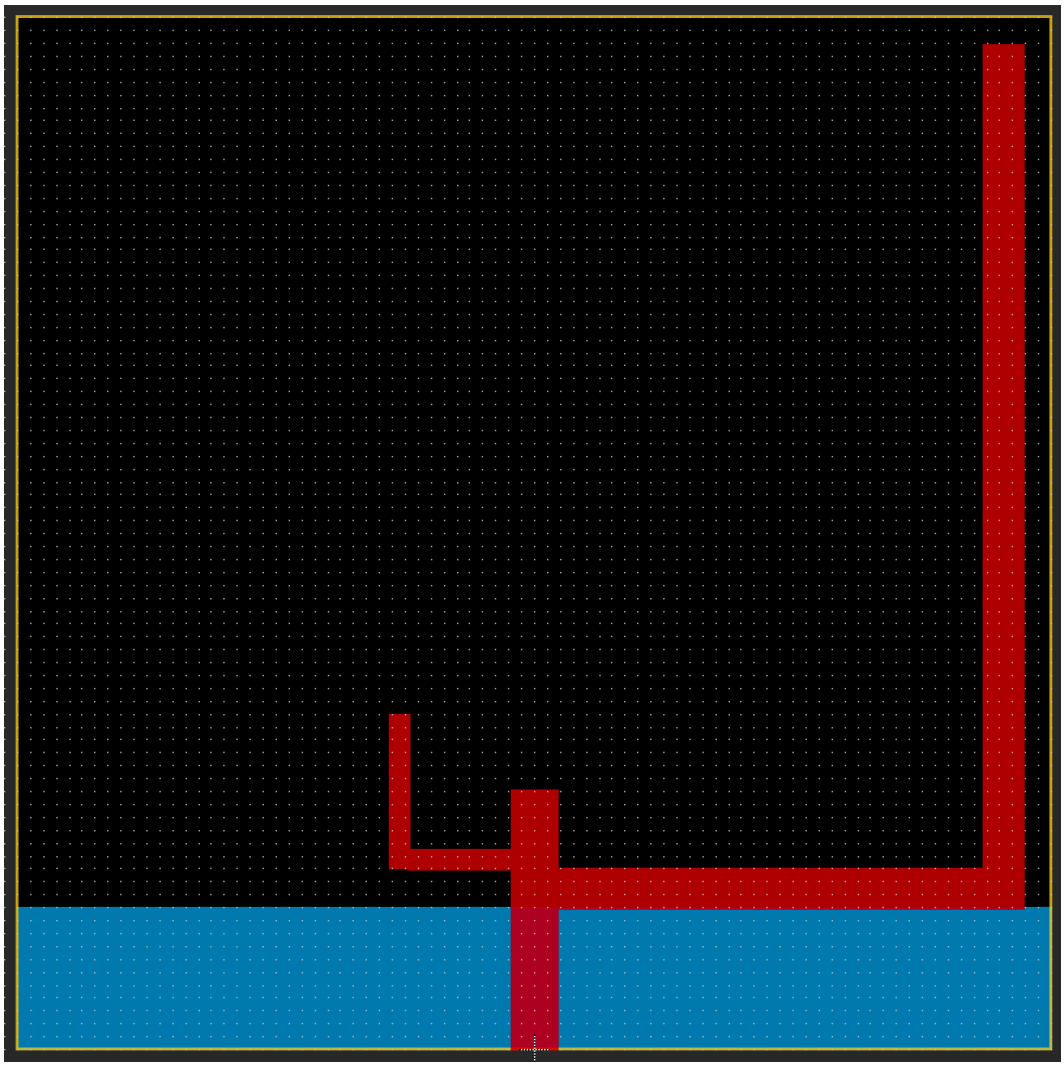

Figure 18 – Top view of the board (red part is conductor, blue part is ground plane)

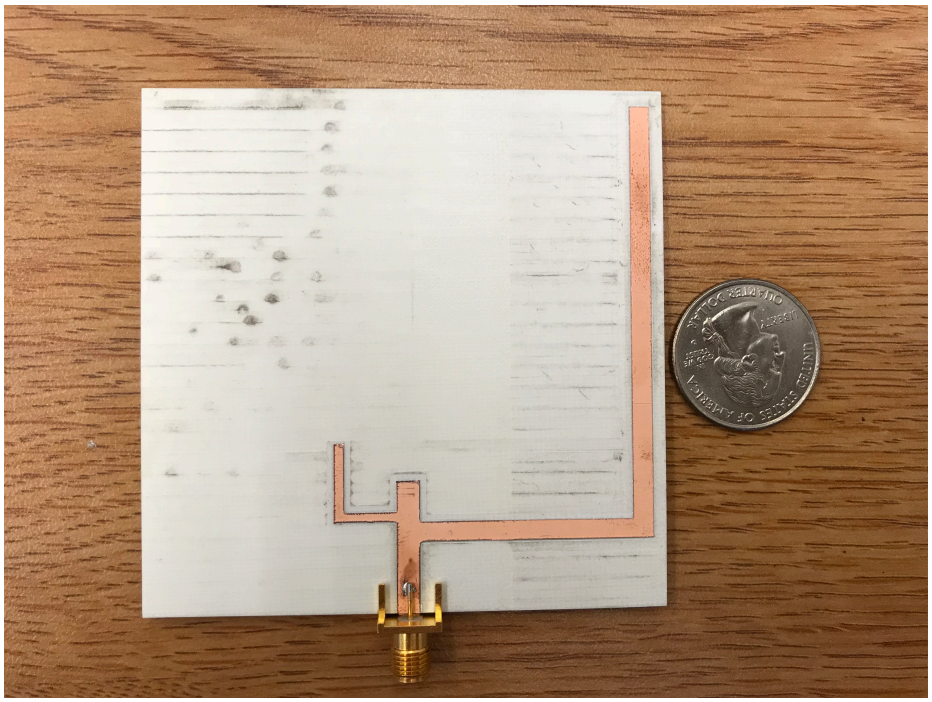

Figure 19 – Photo of the fabricated prototype (Front side). Dielectric substrate is Rogers 4730

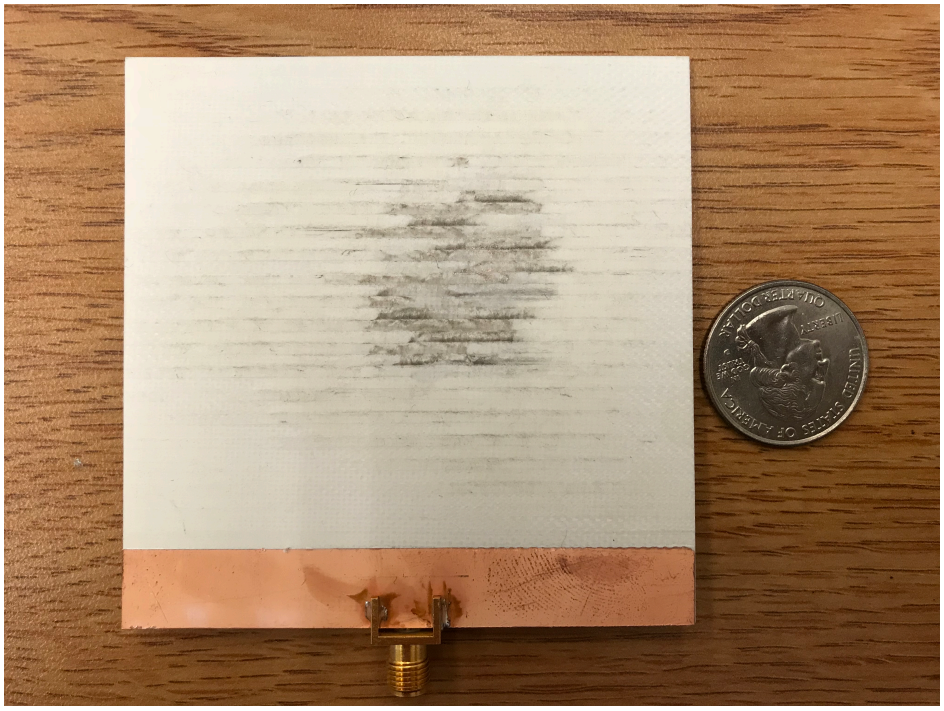

Figure 20 – Photo of the fabricated prototype (Reverse side)

3.2 Results

3.2.1 S-Parameter(S11)

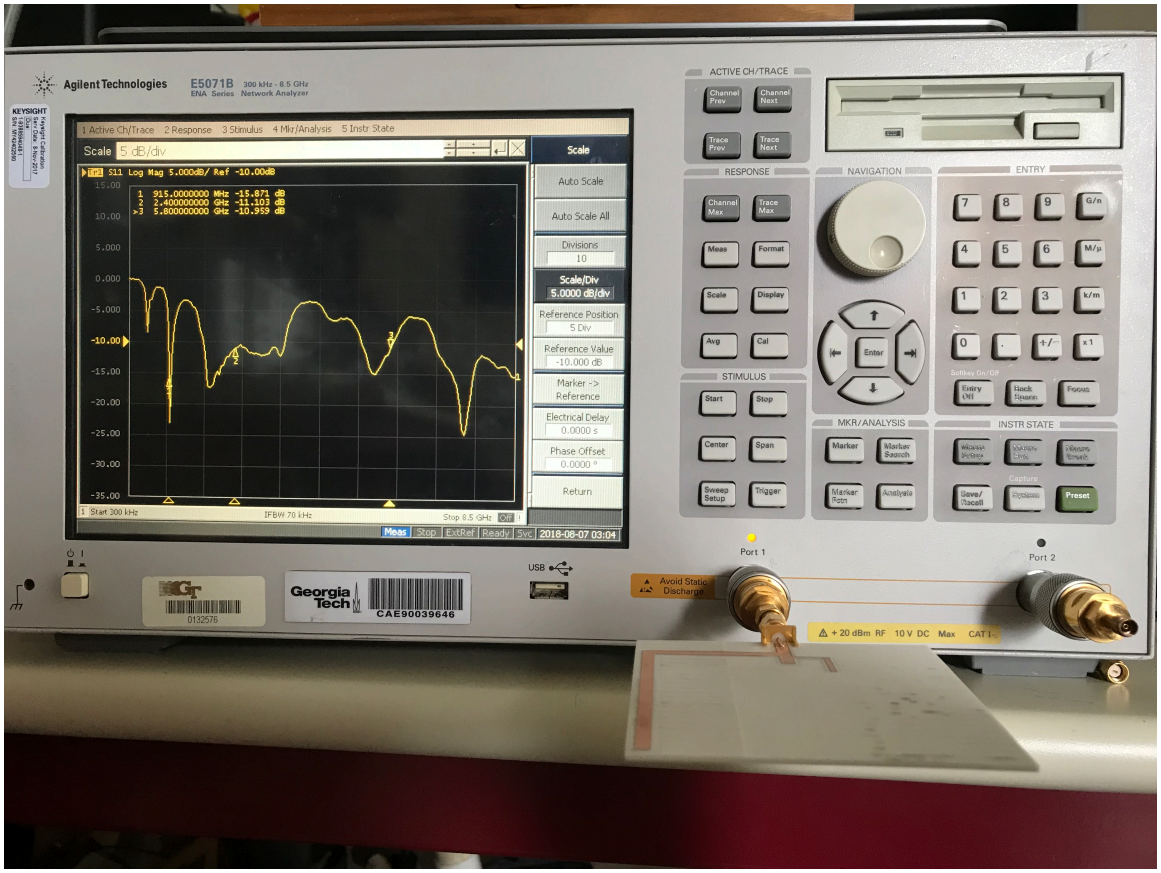

Figure 21 – Testing environment setup

The fabricated prototype is tested and the S-Parameter(S11) is measured with Agilent Technologies E5071B Network Analyzer at room temperature. For calibration process, the 1-port calibration was performed with the Agilent 85033E 3.5mm Calibration Kit. The analyzer sweeps from 300KHz to 8.5GHz and the trace is saved into a csv file. Several python scripts are used to draw the traces and calculate the bandwidth.

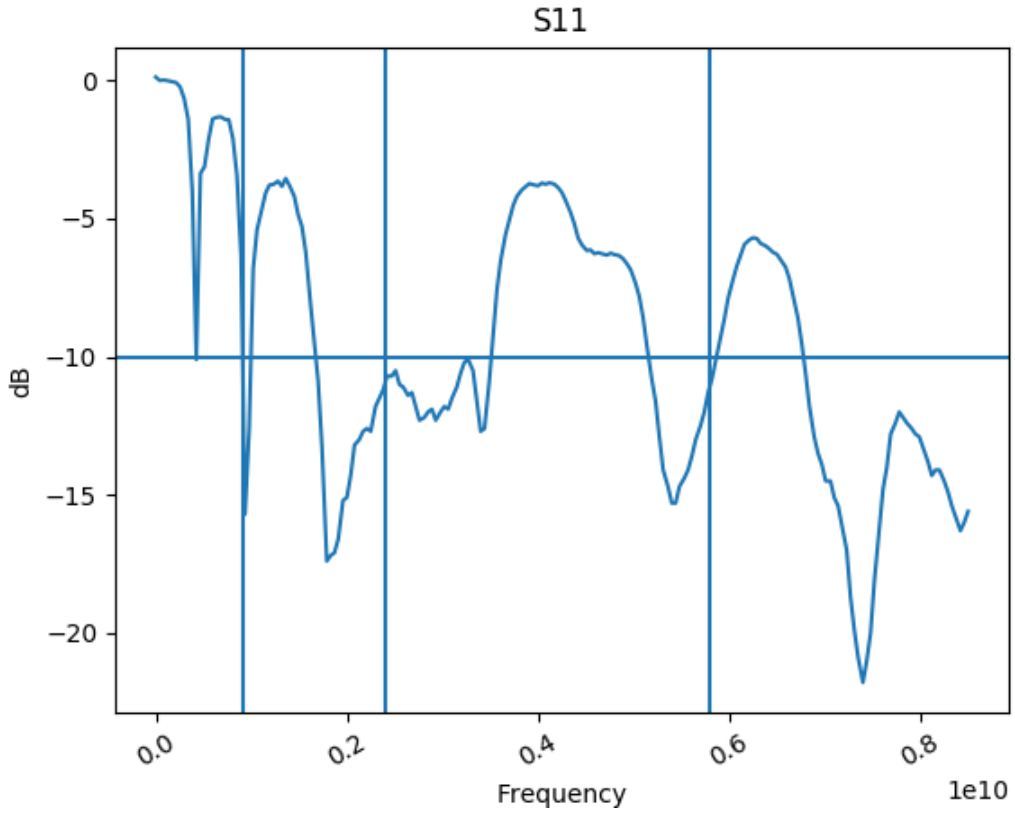

Figure 22 – S-Parameter(S11) measurement for the fabricated prototype antenna across all bands of operation

In Figure 22, the dB marker is set for -10dB and the frequency markers are set for 915MHz, 2.4GHz and 5.8GHz. It can be seen clearly that the S-Parameter(S11) is under the -10dB marker at 2.4GHz and 5.8GHz. In order to get a clearer look at 915MHz and calculate the bandwidths of all the three targeting frequencies, part of the data is selected from the csv file. The results are shown in Figures 22, 23 and 24.

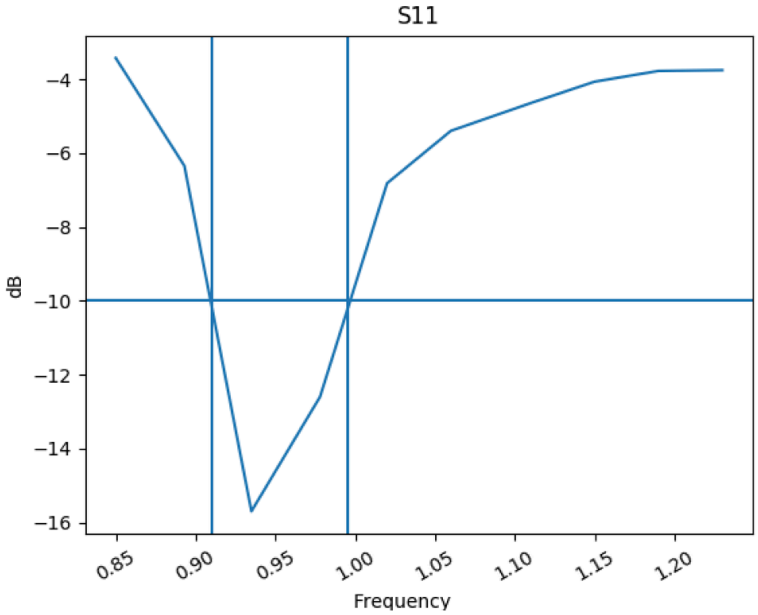

Figure 23 – S-Parameter(S11) measurement for the fabricated prototype antenna around 915MHz

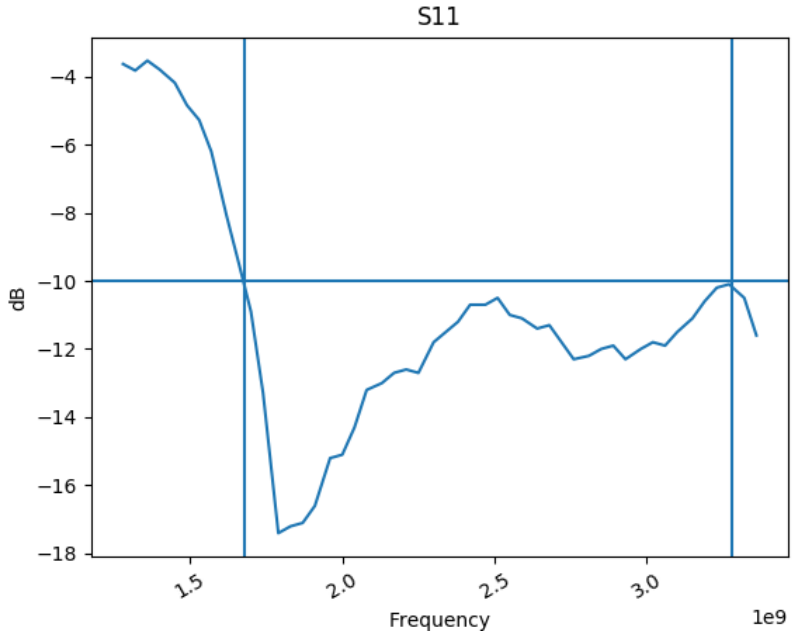

Figure 24 – S-Parameter(S11) measurement for the fabricated prototype antenna around 2.4GHz

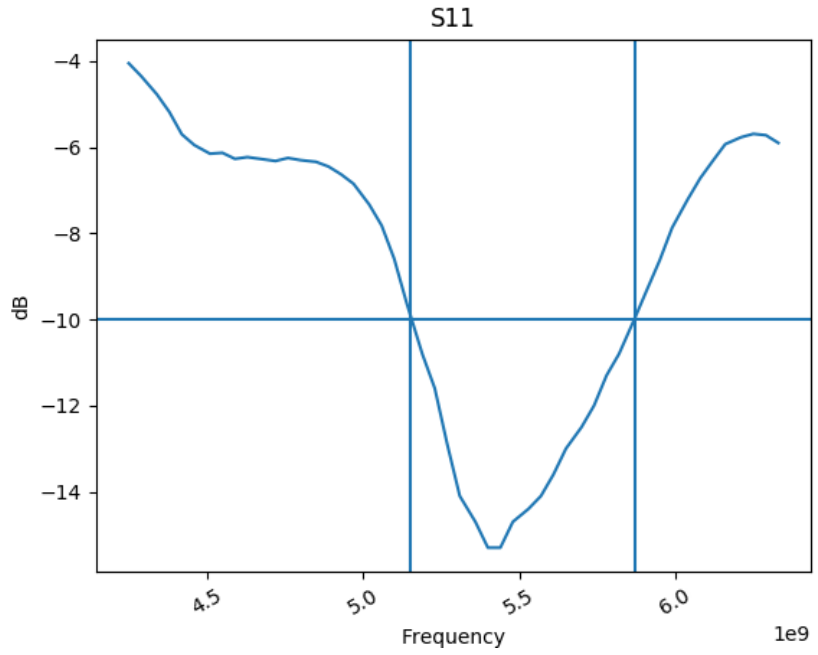

Figure 25 – S-Parameter(S11) measurement for the fabricated prototype antenna around 5.8GHz

There are 201 data points in the csv file for one trace. For 915MHz, the 20th to 30th data points are used. After setting the frequency marker and calculating with python, the band of 915MHz starts from 910MHz and ends at 995MHz. So the bandwidth is 85MHz and the bandwidth ratio is 9.3%.

For 2.4GHz, the 30th to 80th data points are used. After setting the frequency marker and calculating with python, the band of 2.4GHz starts from 1.68GHz and ends at 3.28GHz. So the bandwidth is 1.6GHz and the bandwidth ratio is 66.7%.

For 5.8GHz, the 100th to 150th data points are used. After setting the frequency marker and calculating with python, the band of 5.8GHz starts from 5.15GHz and ends at 5.82GHz. So the bandwidth is 0.72GHz and the bandwidth ratio is 12.4%.

In the simulation, the proposed antenna achieves a bandwidth of 9.8%, 39.1% and 14.1% at each band, respectively. The fabricated prototype achieves local bandwidth of 9.3%, 66.7% and 12.4% at 915MHz, 2.45GHz, and 5.8GHz respectively. For 915MHz and 5.8GHz, the result is quite close the simulation. For 2.4GHz, the S-Parameter(S11) in Figure 14 almost exceeds -10dB which makes the bandwidth (2.5GHz -1.68GHz) / 2.4GHz = 34.2%. It is also quite close to 39.1%. This discrepency may be caused by some noise or some poor connection of the antenna, but it still results in a usable antenna with object resistant properties.

3.2.2 Radiation Pattern

For this part, LabVolt Antenna Training and Measuring System and a ROHDE & SCHWARZ SMB 100A Signal Generator are used. The main elements of the LabVolt system are the Data Acquisition Interface/ Power Supply, the Antenna Positioner and the computer. In order to get the 915MHz radiation pattern for the fabricated prototype, a Yagi antenna is used as a Tx antenna and a 915MHz dipole antenna is used as a reference antenna for calibration. First, an antenna mast with horizontal clips is placed on the transmission support. Then the Yagi antenna is clipped onto it. Next, a long SMA cable on the 1 GHz Oscillator output of the RF Generator is used to connect the Yagi Antenna. For the reference dipole antenna, it is clipped onto the Antenna Positioner and is connected to a 10dB attenuator with a short SMA cable. After all the equipment is set up, the RF Generator and the Power Supply are powered up. Finally, the LVDAM-ANT software is opened and run, and the reference radiation pattern can be saved from the software. Then, the reference antenna is replaced with the fabricated prototype antenna. The LVDAM-ANT software is used to obtain the H-plane and E-plane patterns for comparison with the reference pattern.

For 2.4GHz, the Tx antenna is an E-shaped antenna in [18] and the reference antenna is a probe feed patch antenna whose gain is 4dBi. For 5.8GHz the Tx antenna is an E-shaped antenna and the gain of the reference antenna is 10.3dBi. The results can be seen in Figure 33, 34 and 35. As for the peak gain, the fabricated prototype antenna achieves 2.5dBi, 4dBi and 4.3dBi while the simulated antenna achieves 2dBi, 3dBi and 5dBi for 915MHz, 2.4GHz and 5.8GHz respectively. This discrepency may be caused by some noise or the low accuracy of the testing system, but still results in a usable antenna with enough peak gain.

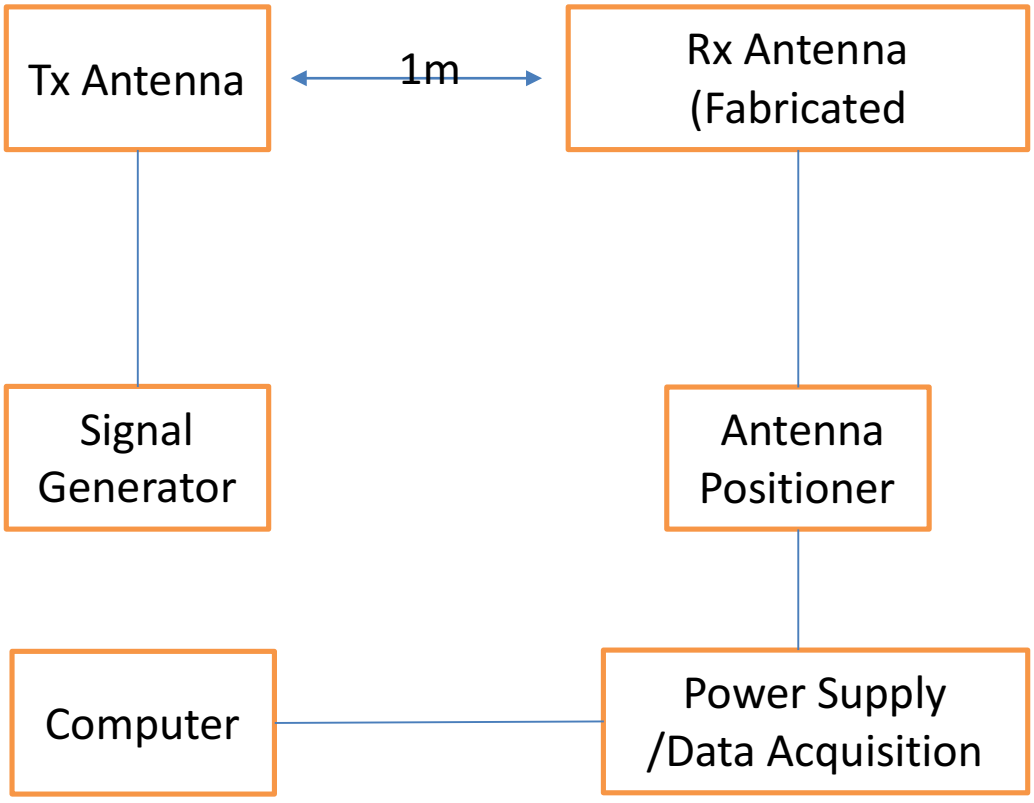

Figure 26 – Testing environment setup block diagram

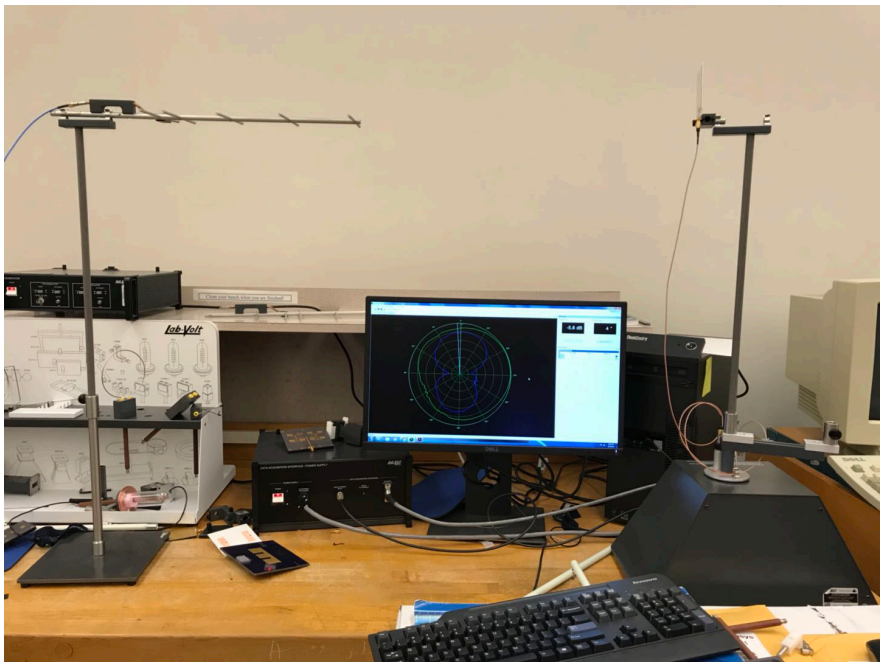

Figure 27 – 915MHz testing environment setup

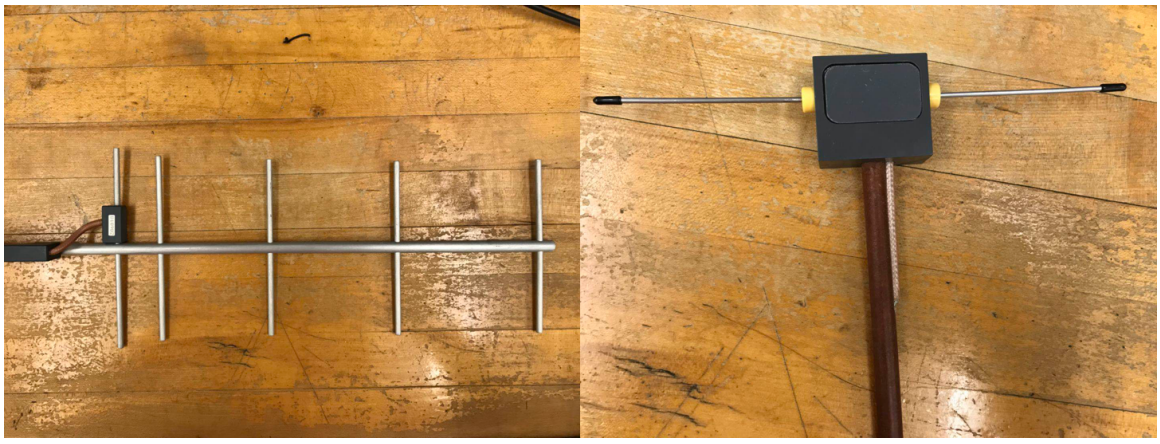

Figure 28 – Tx Antenna(Left) and Reference Antenna(Right) for 915MHz

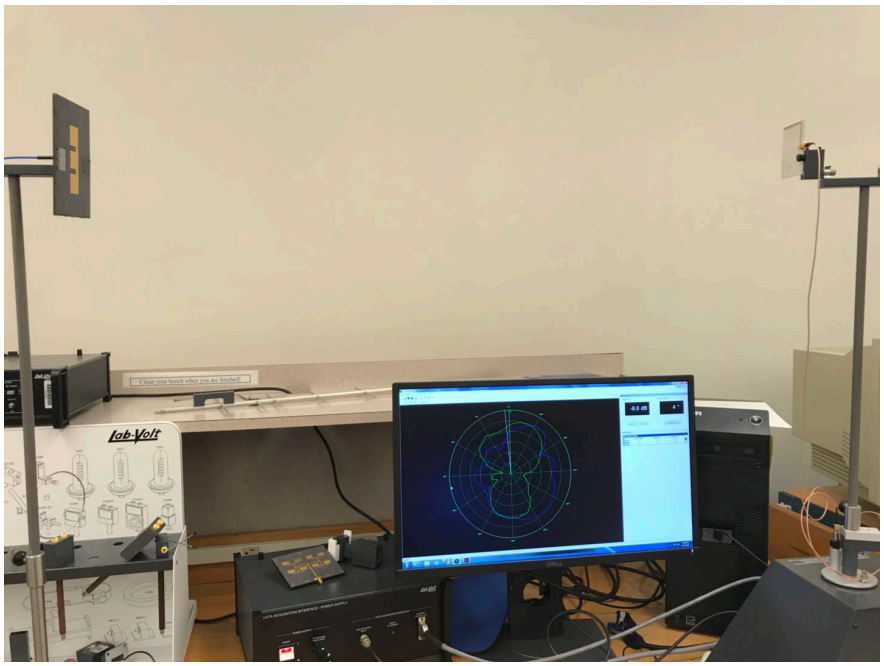

Figure 29 – 2.4GHz testing environment setup

Figure 30– Tx Antenna (Left) [18] and Reference Antenna (Right) for 2.4GHz

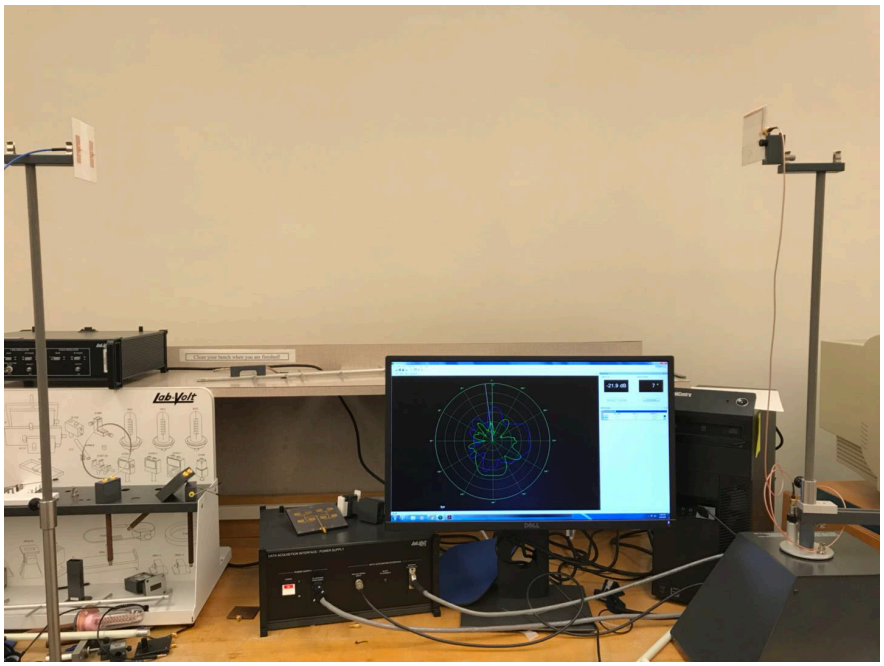

Figure 31 – 5.8GHz testing environment setup

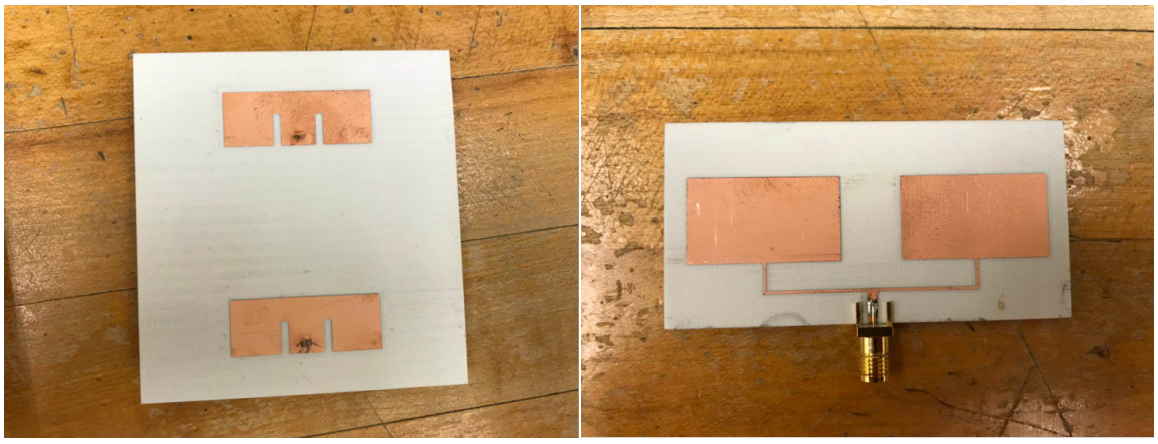

Figure 32- Tx Antenna (Left) and Reference Antenna (Right) for 2.4GHz

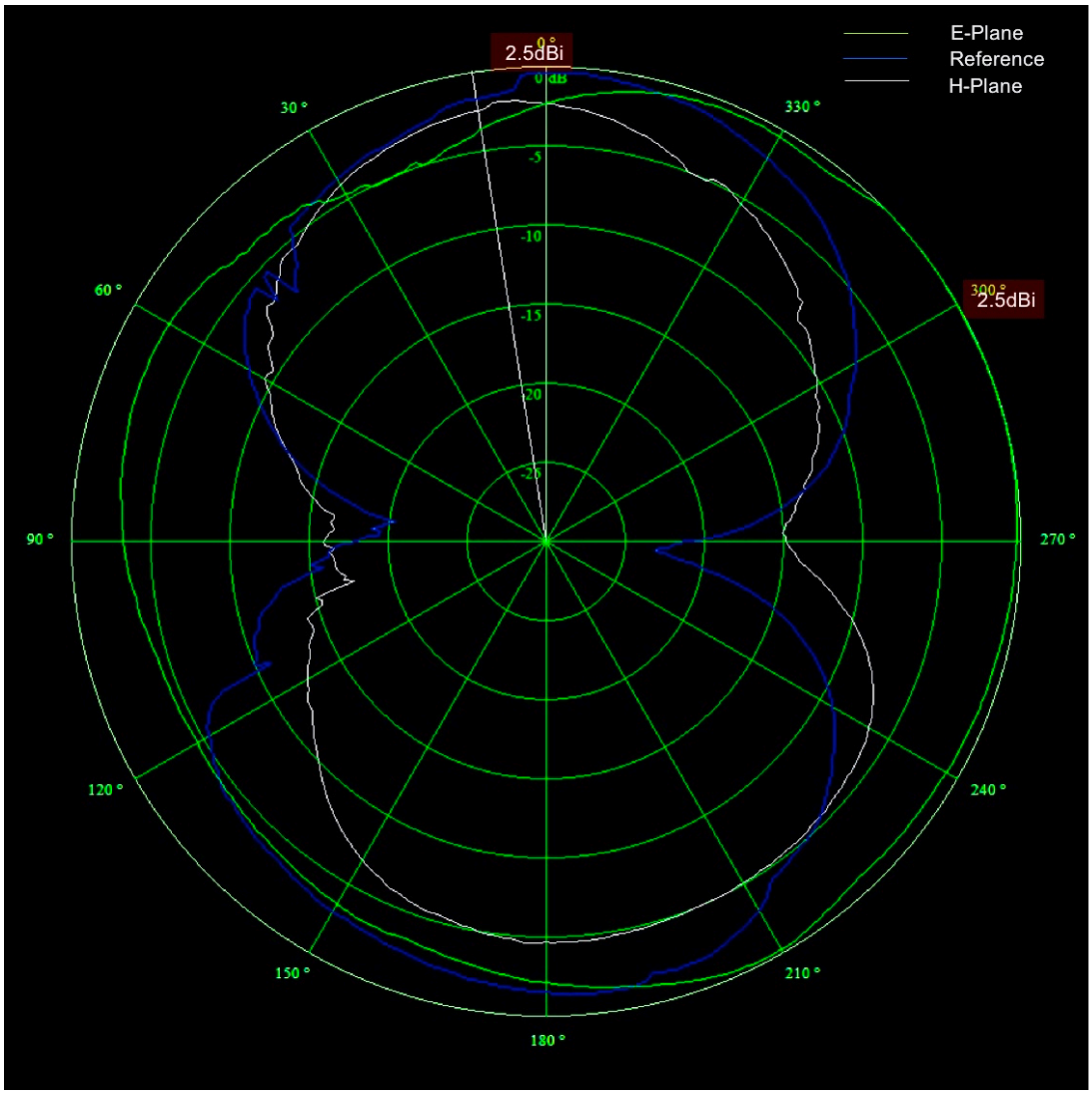

Figure 33 – The Radiation Pattern at 915MHz (Peak Gain 2.5dBi)

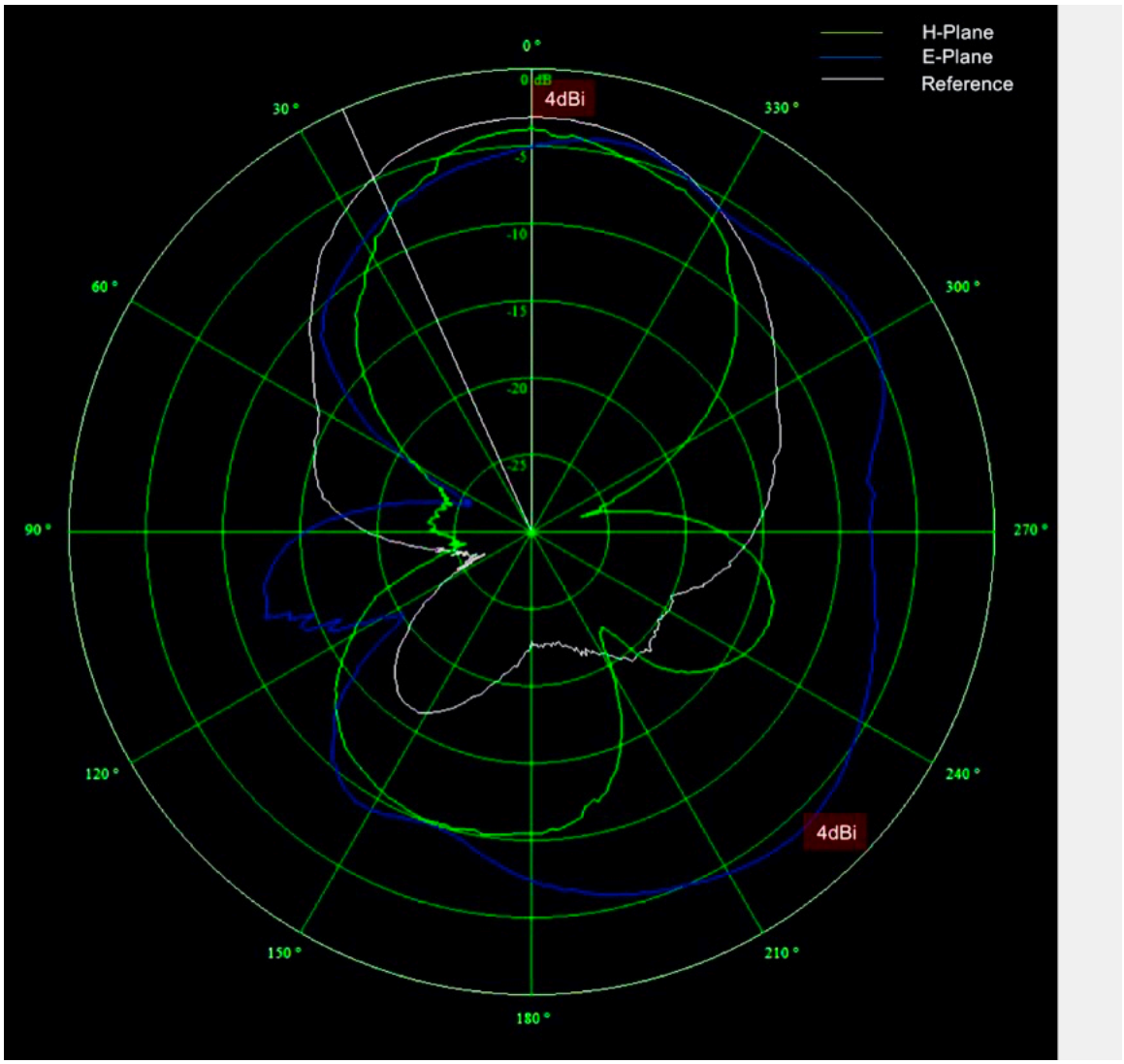

Figure 34 – The Radiation Pattern at 2.4GHz (Peak Gain 4dBi)

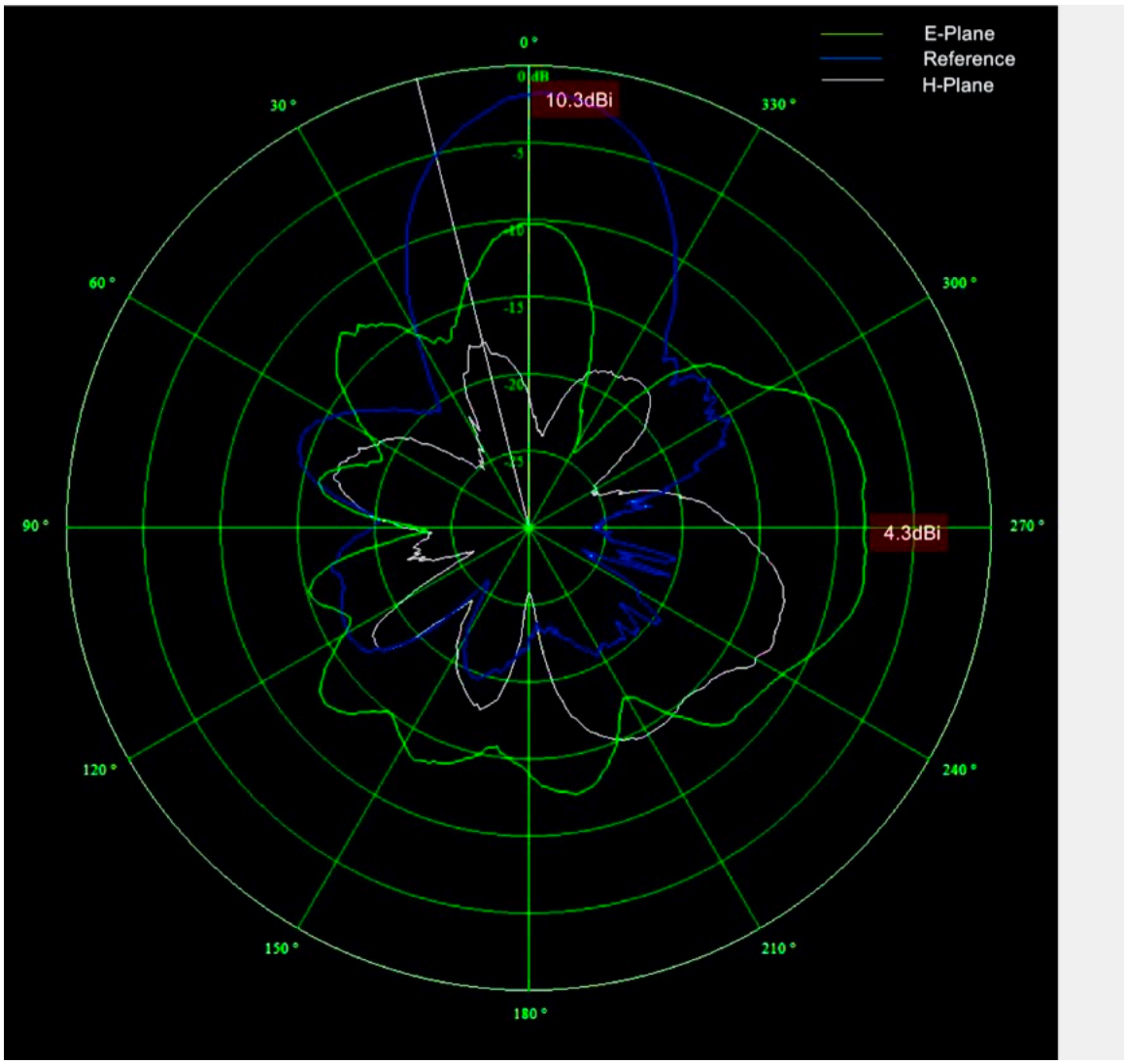

Figure 35 – The Radiation Pattern at 5.8GHz (Peak Gain 4.3dBi)

CHAPTER 4. CONCLUSION

In this paper, a tri-band, object-resistant antenna working at 915MHz, 2.4GHz and 5.8GHz was designed and fabricated. The L-shaped structure was chosen for the purpose of simplicity and convenience of manufacture. At first three L-shaped antennas were designed for three bands, but two were sufficient enough to radiate in all three bands.

Also, in order to be object-resistant, the antenna is designed to be broadband for all the three bands. For 2.4GHz and 5.8GHz the bandwidth ratios are 66.7% and 12.4% respectively, larger than required by US Part 15 device operation. This will afford an additional resistance to object degradation. For 915MHz, the bandwidth is not as wide, so there is still space for improvement in future work.

Not only does this thesis present a useful, tested tri-band ISM antenna for use in numerous radio applications, but presents a powerful design methodology. This methodology can be used to design numerous multiband antennas that can be incorporated into today's electronic devices.

The method of using multiple, higher-band resonances has one key drawback. Because the overall bandwidth increases, there exists the potential for more interference to be received without filtering. This additional potential interference can result in several problems on a modern radio receiver, including overall degradation of carrier-to-interference ratio for the digital detector or saturation of front-end RF electronics in the receive chain. However, all of these detrimental affects can be avoided through the used of careful RF design principles. It is a worthwhile trade-off to handle antenna variations in

this manner and to compensate with additional RF electronic design, where conditions and performance are much more predictable.

APPENDIX A. DESIGN PROPERTIES

Table 2 – Design properties for the dual-band antenna

Design Properties	Value (mm)
H	1.52
S	3.5
L	14
W	2
L1	4.25
L2	7
R1	10.25
R2	19

Table 3 – Final Design Properties

Design Properties	Value (mm)
H	1.524
W	3.5
L	20.2
W1	3.1
W2	1.5
L1	8
L2	12
R1	33
R2	67

APPENDIX B. PYTHON SNIPPETS

```
import pandas as pd
import matplotlib
matplotlib.use('Agg')
import matplotlib.pyplot as plt

trace = pd.read_csv('trace.csv', sep='\s*,\s*',
    header=0, encoding='ascii', engine='python')


plt.plot(trace['Frequency'], trace['Formatted Data'])

plt.xticks(rotation=30)
plt.xlabel('Frequency')
plt.ylabel('dB')
plt.title('S11')

plt.axvline(915000000)
plt.axvline(2400000000)
plt.axvline(5800000000)


plt.axhline(-10)

plt.savefig('All.png')
plt.show()
```

Figure 36 – Draw S-Parameter(S11) with the whole csv file

```
import pandas as pd
import matplotlib
matplotlib.use('Agg')
import matplotlib.pyplot as plt

trace = pd.read_csv('kk.csv', sep='\s*,\s*',
    header=0, encoding='ascii', engine='python')


trace = trace[20:30]

plt.plot(trace['Frequency'], trace['Formatted Data'])

plt.xticks(rotation=30)
plt.xlabel('Frequency')
plt.ylabel('dB')
plt.title('S11')


plt.axvline(910000000)
plt.axvline(995000000)


plt.axhline(-10)

plt.savefig('915MHz.png')
plt.show()
```

Figure 37 – Draw S-Parameter(S11) and show the bandwidth of 915MHz

```
import pandas as pd
import matplotlib
matplotlib.use('Agg')
import matplotlib.pyplot as plt

trace = pd.read_csv('trace.csv', sep='\s*,\s*',
    header=0, encoding='ascii', engine='python')


trace = trace[30:80]

plt.plot(trace['Frequency'], trace['Formatted Data'])

plt.xticks(rotation=30)
plt.xlabel('Frequency')
plt.ylabel('dB')
plt.title('S11')


plt.axvline(1680000000)
plt.axvline(3280000000)


plt.axhline(-10)

plt.savefig('2.4GHz.png')
plt.show()
```

Figure 38 – Draw S-Parameter(S11) and show the bandwidth of 2.4GHz

```
import pandas as pd
import matplotlib
matplotlib.use('Agg')
import matplotlib.pyplot as plt

trace = pd.read_csv('trace.csv', sep='\s*,\s*',
    header=0, encoding='ascii', engine='python')


trace = trace[100:150]

plt.plot(trace['Frequency'], trace['Formatted Data'])

plt.xticks(rotation=30)
plt.xlabel('Frequency')
plt.ylabel('dB')
plt.title('S11')


plt.axvline(5150000000)
plt.axvline(5870000000)


plt.axhline(-10)

plt.savefig('5.8GHz.png')
plt.show()
```

Figure 39 – Draw S-Parameter(S11) and show the bandwidth of 5.8GHz

REFERENCES

[1] Jianjun Li, Lijuan Yu, Wenquan Du " Design of Triple-Band Monopole Antenna for WLAN/WiMAX," Electronic Sci. & Tech., 15 Jan 2013.

[2] C. Qi, M. B. Akbar and G. D. Durgin, "Analysis of E-patch antenna performance over various dielectric materials at 2.4 GHz," *2016 IEEE International Symposium on Antennas and Propagation (APSURSI)*, Fajardo, 2016, pp. 1807-1808.

[3] J. D. Griffin, G. D. Durgin, A. Haldi and B. Kippelen, "RF Tag Antenna Performance on Various Materials Using Radio Link Budgets," in *IEEE Antennas and Wireless Propagation Letters*, vol. 5, pp. 247-250, 2006.

[4] A. Chatterjee, M. Midya and M. Mitra, "Dual-band miniaturized planar inverted F-antenna for WLAN and 5G application," 2017 IEEE Applied Electromagnetics Conference (AEMC), Aurangabad, 2017, pp. 1-2.

[5] I. Dioum, A. Diallo, S. M. Farssi and C. Luxey, "A Novel Compact Dual-Band LTE Antenna-System for MIMO Operation," in *IEEE Transactions on Antennas and Propagation*, vol. 62, no. 4, pp. 2291-2296, April 2014.

[6] N. Kathuria and S. Vashisht, "Dual-band printed slot antenna for the 5G wireless communication network," *2016 International Conference on Wireless Communications, Signal Processing and Networking (WiSPNET)*, Chennai, 2016, pp. 1815-1817.

[7] A. Shafqat and F. A. Tahir, "Miniaturized tapered meandered dual band dipole antenna for WiFi 2.4/5.8 GHz application," 2017 Progress in Electromagnetics Research Symposium - Fall (PIERS - FALL), Singapore, 2017, pp. 1640-1642.

[8] L. Tian, Z. Xue, W. Li and W. Ren, "Stacked tri-band microstrip patch antenna," 2017 IEEE 5th International Symposium on Electromagnetic Compatibility (EMC-Beijing), Beijing, 2017, pp. 1-3.

[9] S. K. Veeravalli, K. Shambavi and Z. C. Alex, "Design of tri band antenna for mobile handset applications," 2013 International Conference on Communication and Signal Processing, Melmaruvathur, 2013, pp. 947-950.

[10] Ray, Dr & Thakur, Sanjay & Deshmukh, R.A.. (2012). Wideband L-shaped printed monopole antenna. AEU - International Journal of Electronics and Communications. 66. 693–696. 10.1016/j.aeue.2011.12.012.

[11] Hua-Ming Chen and Yi-Fang Lin, "Printed monopole antenna for 2.4/5.2 GHz dual-band operation," IEEE Antennas and Propagation Society International Symposium. Digest. Held in conjunction with: USNC/CNC/URSI North American Radio Sci. Meeting (Cat. No.03CH37450), Columbus, OH, USA, 2003, pp. 60-63 vol.3.

[12] C. A. Balanis, Antenna Theory: Analysis and Design, New York:Wiley, 1982

[13] ARTICLE 1 - Terms and Definitions". life.itu.ch. International Telecommunication Union. 19 October 2009. 1.15. industrial, scientific and medical (ISM) applications (of radio frequency energy): Operation of equipment or appliances designed to generate and use locally radio 5 frequency energy for industrial, scientific, medical, domestic or similar purposes, excluding applications in the field of telecommunications.

[14] “Unlicensed 915-MHz Band Fits Many Applications and Allows Higher Transmit Power.” Improving the Efficiency of LED Light Emission | DigiKey, www.digikey.com/en/articles/techzone/2011/may/unlicensed-915-mhz-band-fits-many-applications-and-allows-higher-transmit-power.

[15] “List of 2.4 GHz Radio Use.” Wikipedia, Wikimedia Foundation, 17 July 2018, en.wikipedia.org/wiki/List_of_2.4_GHz_radio_use.

[16] "ISM Band. " Wikipedia, Wikimedia Foundation, 23 July 2018, en.wikipedia.org/wiki/ISM_band.

[17] M. Zhang, G. Luo, L. Feng and L. Kui, "A novel dual-band planar monopole mobile phone antenna for TD-LTE and TD-SCDMA applications," 2017 4th International Conference on Systems and Informatics (ICSAI), Hangzhou, 2017, pp. 906-910.

[18] C. Qi, M. B. Akbar and G. D. Durgin, "Analysis of E-patch antenna performance over various dielectric materials at 2.4 GHz," *2016 IEEE International Symposium on Antennas and Propagation (APSURSI)*, Fajardo, 2016, pp. 1807-1808